Biogeosciences

Geomorphologic controls and anthropogenic impacts on dissolved organic carbon from mountainous rivers: insights from optical properties and carbon isotopes

Shuai Chen[1], **Jun Zhong**[2], **Lishan Ran**[1], **Yuanbi Yi**[2], **Wanfa Wang**[3], **Zelong Yan**[4], **Si-liang Li**[2,5], **and Khan M. G. Mostofa**[2]

[1]Department of Geography, The University of Hong Kong, Pokfulam Road, Hong Kong, China
[2]Institute of Surface-Earth System Science, School of Earth System Science, Tianjin University, Tianjin, 300072, China
[3]College of Resources and Environmental Engineering, Key Laboratory of Karst Georesources and Environment, Ministry of Education, Guizhou University, Guiyang, 550025, China
[4]School of Environmental Science and Technology, Dalian University of Technology, Dalian, 116081, China
[5]State Key Laboratory of Hydraulic Engineering Simulation and Safety, Tianjin University, Tianjin 300072, China

Correspondence: Jun Zhong (jun.zhong@tju.edu.cn) and Lishan Ran (lsran@hku.hk)

Abstract. Mountainous rivers are critical in transporting dissolved organic carbon (DOC) from terrestrial environments to downstream ecosystems. However, how geomorphologic factors and anthropogenic impacts control the composition and export of DOC in mountainous rivers remains largely unclear. Here, we explore DOC dynamics in three subtropical mountainous catchments (i.e., the Yinjiang, Shiqian, and Yuqing catchments) in southwest China, which are heavily influenced by anthropogenic activities. Water chemistry, stable and radioactive carbon isotopes of DOC ($\delta^{13}C_{DOC}$ and $\Delta^{14}C_{DOC}$), and optical properties (UV absorbance and fluorescence spectra) were employed to assess the biogeochemical processes and controlling factors on riverine DOC. The radiocarbon ages of DOC in the Yinjiang River varied widely from 928 years BP to the present. Stepwise multiple regression analyses and partial least square path models revealed that geomorphology and anthropogenic activities were the major drivers controlling DOC concentrations and DOM characteristics. Catchments with higher catchment slope gradients were characterized by lower DOC concentrations, enriched $\delta^{13}C_{DOC}$ and $\Delta^{14}C_{DOC}$, and more aromatic dissolved organic matter (DOM), which were opposite to catchments with gentle catchment slopes. Variabilities in DOC concentrations were also regulated by land use, with higher DOC concentrations in urban and agricultural areas. Furthermore,

DOM in catchments with a higher proportion of urban and agricultural land uses was less aromatic, less recently produced, and exhibited a higher degree of humification and more autochthonous humic-like DOM. This research highlights the significance of incorporating geomorphologic controls on DOC sources and anthropogenic impacts on DOM composition into the understanding of DOC dynamics and the quality of DOM in mountainous rivers, which are globally abundant.

1 Introduction

Dissolved organic carbon (DOC) plays a fundamental role in the riverine carbon cycle with approximately 0.26 Pg (1 Pg $= 10^{15}$ g) of DOC exported from global rivers to the ocean each year, accounting for more than half of the total organic carbon export (Cai, 2011; Raymond and Spencer, 2015). In view of continued climate warming and rapid land use changes, it is important to gain a better understanding of the spatial and temporal dynamics of DOC transport in river systems (Butman et al., 2014; Fasching et al., 2016; Zhong et al., 2021). For example, elevated temperature has a dominant effect on DOC concentration and dissolved organic matter (DOM) composition by enhancing decomposition and

photochemical degradation rates of DOM (Zhou et al., 2018), thereby contributing to significant CO_2 emissions from inland waters (Raymond et al., 2013). Additionally, DOM provides energy and nutrient sources for aquatic biota (Findlay et al., 1998), adsorbing heavy metals and organic pollutants (Aiken et al., 2011). Riverine DOC can also restrict in-stream primary production by reducing light penetration and lowering temperature in the water column, thereby serving as an important determinant in shaping the ecological and biogeochemical processes in aquatic environments (Ask et al., 2009). Therefore, disentangling the processes controlling riverine DOC dynamics is crucial for a greater understanding of aquatic ecosystem functioning and the global carbon cycle. Recent advances in spectroscopic techniques, especially the UV-visible spectrophotometry and fluorescence spectroscopy, and widespread application of stable and radioactive carbon isotopes on bulk DOC have provided insights into the composition, source, and age of DOM in freshwater ecosystems (Fellman et al., 2010; Marwick et al., 2015; Minor et al., 2014). These new techniques have led to significant improvements in our understanding of the biogeochemical processes of DOC in river systems, which will continue to be effective tools for researchers to gain deeper insights into the riverine carbon cycle.

The biogeochemical processes of DOM in river systems have been extensively studied, and they depend largely on the sources and composition of DOM (Toming et al., 2013). Riverine DOM is a mixture generated from autochthonous and allochthonous sources. Among them, autochthonous DOM is a pool of dead and living microbial and algal biomass that is derived within the aquatic ecosystem (Devesa-Rey and Barral, 2011), which mainly consists of non-humic substances that are more bioavailable (Toming et al., 2013). By comparison, allochthonous DOM refers to DOM that originates from outside of the aquatic ecosystem and is typically composed of higher plant and soil organic matter (Zhang et al., 2023), which may also contain organic waste of anthropogenic origin (Ramos et al., 2006; Toming et al., 2013). Consequently, allochthonous DOM is generally characterized by high lignin content and high molecular weight, making it refractory to decomposition (Devesa-Rey and Barral, 2011).

Recent studies have indicated the significance of geomorphologic factors, such as elevation and catchment slope, in influencing the export of DOC and riverine carbon cycling (Connolly et al., 2018; Li Yung Lung et al., 2018). Compared with high-relief catchments, low-relief regions with longer water residence time, stronger hydrologic connectivity to rivers, and greater development of wetlands are typically characterized by increased concentration of riverine DOC (Harms et al., 2016; McGuire et al., 2005). Specifically, DOC supply is probably regulated by the amount of stored soil organic carbon (SOC) in a catchment (Lee et al., 2019; Rawlins et al., 2021). However, this supply is limited by shallow soil depth and high flow velocity in high-relief

regions (Lee et al., 2019). The varying extent of hydrologic connectivity due to changing water residence time with different catchment slopes may also have significant influences on DOC dynamics (Connolly et al., 2018). Typically, it is anticipated that as the slope increases toward higher elevation areas, where residence time is relatively short and soil organic matter is well connected to hydrologic pathways, the composition of DOM pools in inland waters will shift toward a more "terrestrial" characteristic. This shift involves larger molecules with high molecular weight and aromatic structures (Creed et al., 2018; Xenopoulos et al., 2021). Although geomorphologic characteristics have proved to be useful in estimating DOC concentrations (Harms et al., 2016; Mzobe et al., 2020), the underlying mechanisms that regulate DOC dynamics in small mountainous rivers remain poorly understood. Therefore, a deeper understanding of the geomorphologic controls on DOC dynamics is urgently needed. Subtropical small mountainous rivers are characterized by steep catchment slopes, high erosion rates, frequent rainfall events in wet seasons, and rapid change in hydrology during these rainfall events (Lee et al., 2019; Leithold et al., 2006), yet have received little research attention regarding their DOC dynamics. Moreover, runoff, catchment slope gradient, and SOC have been recognized as good predictors for DOC export in small mountainous rivers (Lee et al., 2019). Yet, the extent to which these factors, along with land use patterns, effectively regulate the DOC dynamics is still far from well understood (Lee et al., 2019; Moyer et al., 2013).

Anthropogenic impacts, such as urban and agricultural land uses, have led to significant alterations in the flux of DOC and the fate and quality of DOM in global streams and rivers (Coble et al., 2022; Wilson and Xenopoulos, 2008; Xenopoulos et al., 2021). Agricultural streams and rivers are dominated by microbial-derived, protein-like DOM, while urban freshwater ecosystems are characterized by microbial, humic-like or protein-like, and autochthonous DOM (Hosen et al., 2014; Williams et al., 2016; Xenopoulos et al., 2021). Agricultural and urban land uses tend to increase nutrient loading in streams, resulting in enhanced bacterial production and DOM decomposition (Quinton et al., 2010; Williams et al., 2010). As a result, microbial-derived DOM plays a crucial role in agricultural and urban rivers. In addition, DOM tends to have a more reduced redox state and is likely more labile and accessible to the microbial community in agricultural streams when compared to the DOM found in natural streams (Fasching et al., 2019; Williams et al., 2010). On the scale of years to decades, anthropogenic impacts can accelerate terrestrially sourced DOC export to aquatic ecosystems (Xenopoulos et al., 2021). On the scale of decades to centuries, however, anthropogenic impacts would shift natural DOM to forms of low molecular weight, enhanced redox state with potentially increased liability, or increased aromaticity due to warmer climate and altered hydrology (Stanley et al., 2012; Xenopoulos et al., 2021).
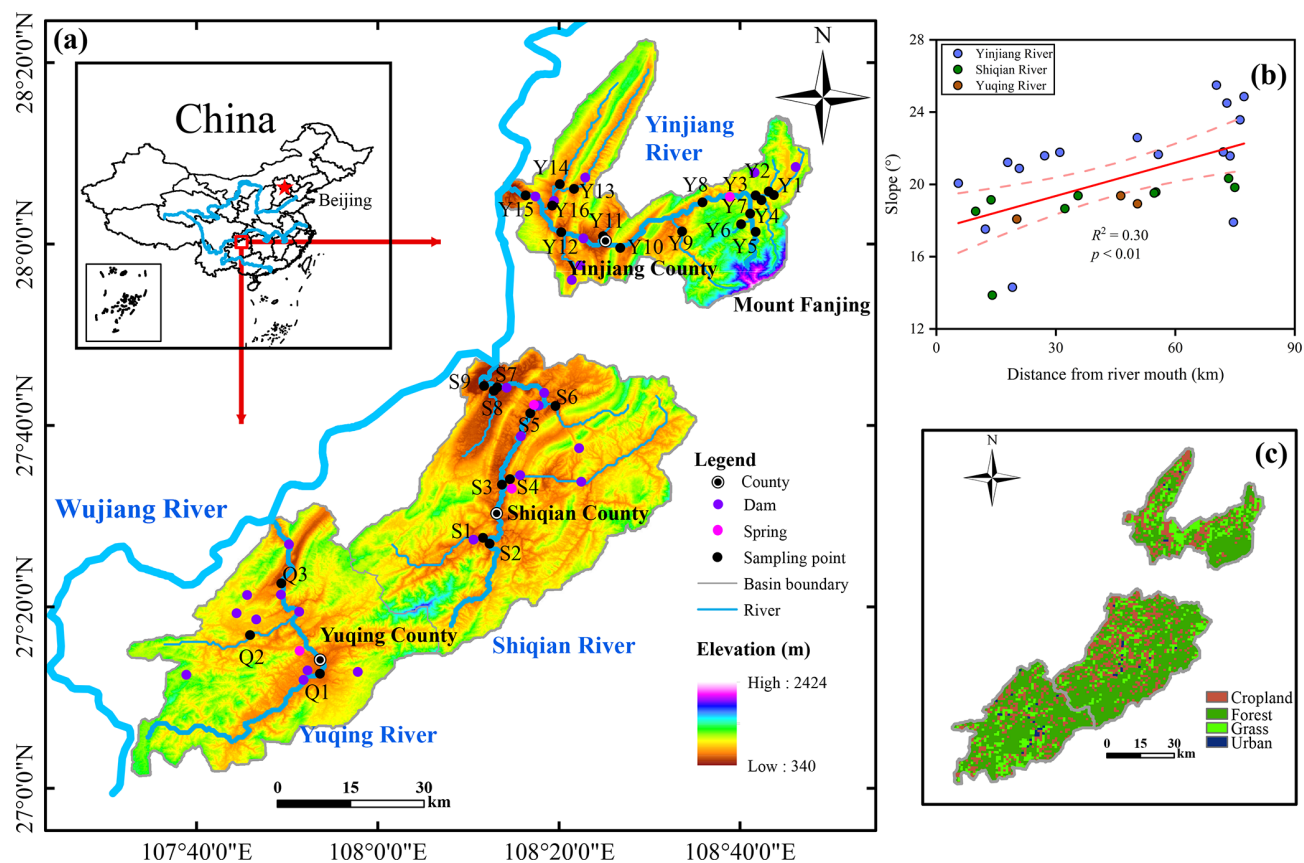
Figure 1. Map of the study area. **(a)** Overview of the sampling sites and elevation characteristics in the three study catchments, including the Yinjiang, Shiqian, and Yuqing catchments, **(b)** correlation between mean catchment slope and the distance from the river mouth (i.e., the Yinjiang, Shiqian, and Yuqing rivers) to the sampling site, and **(c)** spatial variation in land use patterns.

In this study, we evaluated how geomorphologic controls (i.e., mean catchment slope and mean drainage elevation) and anthropogenic impacts (i.e., land use patterns) affect the DOC dynamics and DOM characteristics in three subtropical catchments encompassing numerous small-to-medium mountainous rivers in southwest China. Our prior observations from these catchments showed that particulate organic carbon (POC) and dissolved inorganic carbon (DIC) dynamics were highly affected by in-stream photosynthesis, as evidenced by stable carbon isotope and radioactive carbon isotope of POC and DIC (Chen et al., 2021). We hypothesize that catchments with a higher proportion of agricultural and urban land use, gentler catchment slope, and lower elevation would exhibit higher riverine DOC concentrations and more autochthonous microbial humic-like DOM than steeper catchments at high elevations with fewer influences by agricultural and urban land uses. Relationships of DOC concentrations, stable isotopic values of DOC, DOM quality assessed through optical metric, nutrient concentrations, and land use patterns versus geomorphologic characteristics (i.e., mean catchment slope and mean drainage elevation) were examined. We also examined relationships between ge-

omorphologic characteristics and radiocarbon for nine sampling sites in the Yinjiang River. This study allows us to gain deeper insight into the geomorphologic controls and anthropogenic impacts on DOC dynamics and DOM quality in the subtropical, anthropogenically influenced mountainous rivers.

2 Materials and methods

2.1 Study area

The Yinjiang River (Y), Shiqian River (S), and Yuqing River (Q) are tributaries of the Wujiang River (Fig. 1a), the largest tributary on the south bank of the upper Changjiang River. The drainage area is 1231, 2101, and 1561 km^2 for the Yinjiang, Shiqian, and Yuqing rivers, respectively. Data on land use types and air temperature in 2015, as well as a 90 m digital elevation model (Shuttle Radar Topography Mission, SRTM), were obtained from the Resource and Environment Data Cloud Platform of the Chinese Academy of Sciences (http://www.resdc.cn/, last access: 6 February 2023). The SOC content in the surface layer (0–5 cm) was collected from

the SoilGrids1km database (a global soil information system at 1 km resolution) (Hengl et al., 2014). Information on dams was retrieved from Wang et al. (2022), and their location was identified by Google Earth. Furthermore, the distance from the river mouth (i.e., the Yinjiang, Shiqian, and Yuqing rivers) to the sampling sites was also estimated using Google Earth. We further delineated the sub-catchments, which constitute the contributing area upstream of sampling sites, by spatial analyst tools of ArcGIS (version 10.2). The mean catchment slope (degrees; 3D analysis tools) and elevation for sub-catchments were extracted from the digital elevation model using ArcGIS. Annual air temperature (T_{air}), catchment slope, topsoil SOC, and proportion of urban and agricultural land uses for these sub-catchments were also determined using ArcGIS. The mean drainage elevation of these three catchments ranges from 340 m to 2424 m, with the lowest and highest elevations both reported in the Yinjiang River catchment, showing the greatest change in relief (Figs. 1a and S1a in the Supplement). The topsoil SOC exhibited a spatial distribution that resembled elevation, with regions with higher elevation displaying higher SOC contents (Fig. S2 in the Supplement). Similar to elevation, the Yinjiang River catchment has a greater variation in mean catchment slope (from 14.3 to 25.5°), while the Shiqian and Yuqing river catchments have a mean catchment slope of approximately 20°, except the segment above site S8 (13.9°; Figs. 1b and S1b). Carbonate rock is widely distributed in the three catchments, accounting for a large proportion of the exposed strata (Han and Liu, 2004). The remaining areas are mainly covered by clastic rocks, igneous rocks, and low-grade metamorphic rocks. Forest, agriculture, and urban areas are the three dominant land uses in these studied catchments (Fig. 1c). Forest is generally distributed in high-elevation regions, while urban and agricultural land uses are mainly located in low-elevation regions. The proportion of urban and agricultural land uses in the Yuqing River catchment varies from 17.3 % to 23.1 % (Figs. 1c and S1c). This catchment has a higher % urban/agriculture land use than other studied catchments and less variability in land use compared to the Yinjiang and Shiqian river catchments (from 4.5 % to 46.5 % and from 9.6 % to 41.3 %, respectively). There are three mountainous agricultural counties (i.e., Yinjiang, Shiqian, and Yuqing; Fig. 1a) in this study area, where crops are mainly C4 (e.g., corn and sorghum) and C3 (e.g., rice, wheat, and potato) plants. Dams and reservoirs are widely distributed in the three catchments, and these dams are primarily used for agricultural irrigation and power generation (Fig. 1a). This study area is highly affected by monsoon-influenced humid subtropical climate with April to October being the rainy season, and the average annual precipitation, runoff, and discharge are 1100 mm, 1004 mm yr^{-1} and 14.4 m^3 s^{-1}, respectively, in the Yinjiang River catchment. Further details on the regional setting of the study area and the sources and methods for delineation of catchment characteristics are provided in our previous study (Chen et al., 2021).

2.2 Field sampling

Surface water samples ($n = 28$) along the mainstem and major tributaries of the Yinjiang River, Shiqian River, and Yuqing River and spring water samples ($n = 4$) were collected in September 2018 (Fig. 1a). During the sampling period, two water samples (sites Y12 and Y15) were significantly affected by rainfall events, and an additional sample was collected at site Y12 before the rainfall event as it is close to the hydrological station. Unless stated otherwise, the data used in this study from site Y12 are based on the sample collected after rainfall events due to the availability of carbon isotopes. Electrical conductivity (EC) and dissolved oxygen (DO) were measured by a multi-parameter water quality probe (WTW, pH 3630/Cond 3630, Germany) in the field. For the analysis of ion concentrations, total phosphorus (TP), ammonium (NH$_4^+$-N), and total nitrogen (TN), water samples were filtered through 0.45 μm cellulose acetate membranes. Water samples for the concentrations and isotopes of DOC and DOM absorbance and fluorescence were filtered through pre-combusted glass fiber filters (Whatman, 0.7 μm). The filtered water was stored in a Milli-Q water and sampling water pre-washed brand-new low-density polyethylene container at low temperature (4 °C) in the dark during 1–7 d before analysis of optical properties and was acidified by phosphoric acid to pH = 2 for DOC analysis. Water samples were also filtered to determine DIC (through 0.45 μm cellulose acetate membranes) through titration with hydrochloric acid and to analyze POC using retained suspended particles on the filter membranes. The water samples filtered through 0.22 μm cellulose acetate filter membranes were used to determine water isotopes (δ^{18}O and δD). Detailed information on the sampling methods was provided by Chen et al. (2021) and Zhong et al. (2020).

2.3 Laboratory analysis

The main cations (K$^+$, Na$^+$, Ca^{2+}, and Mg^{2+}) were measured by inductively coupled plasma emission spectrometry (ICP-OES), and the main anions (Cl$^-$, SO$_4^{2-}$, and NO$_3^-$) were measured by ion chromatography (Thermo Aquion; Chen et al., 2020). The normalized inorganic charge balance is within 5 %, indicating the accuracy of the measured data. The concentrations of NH$_4^+$-N were analyzed using an automatic flow analyzer (Skalar Sans Plus Systems), and the relative deviations of the results of NH$_4^+$-N were less than 5 %. DOC concentrations were determined with a total organic carbon analyzer (OI Analytical, Aurora 1030W, USA) with duplicates ($\pm$ 1.5 %, analytical error) and a detection limit at 0.01 mg L^{-1}. Water isotopes were measured by a liquid water isotope analyzer (Picarro L2140-i, USA) with measurement precision at $\pm$ 0.3 ‰ for δ^{18}O. The aforementioned analyses

were carried out at the Institute of Surface Earth System Science, Tianjin University.

For the determination of stable carbon isotope and radiocarbon isotope of DOC ($\delta^{13}C_{DOC}$ and $\Delta^{14}C_{DOC}$), water samples were first concentrated using a rotary evaporation and then oxidized through the wet oxidation method (Leonard et al., 2013). In this study, nine water samples collected from the Yinjiang River were selected for $\Delta^{14}C_{DOC}$ analysis as the Yinjiang River catchment has the greatest change in geomorphologic characteristics (i.e., elevation and catchment slope) and the highest proportion of agricultural and urban land uses among the three catchments. The generated CO_2 was purified in a vacuum system for $\delta^{13}C_{DOC}$ and $\Delta^{14}C_{DOC}$ analyses. $\delta^{13}C_{DOC}$ was directly determined using the MAT 253 mass spectrometer with an analysis accuracy of $\pm 0.1\%$. For $\Delta^{14}C_{DOC}$ analysis, the purified CO_2 was transformed into graphite following the same method as for $\Delta^{14}C_{POC}$ analysis (Chen et al., 2021) and measured with an accelerator mass spectrometry (AMS) system within 24 h with an analytical error of $\pm 3\%$ (Dong et al., 2018).

Optical analyses of DOM were conducted on river samples. DOM absorbance of river water samples was measured from 250 to 750 nm at 1 nm intervals using a UV (ultraviolet)-visible spectrophotometer (UV-2700, Shimadzu) with a 1 cm quartz cuvette. The UV-visible spectrophotometer was blanked with Milli-Q water prior to data collection. Decadic absorbance values were used to calculate decadic absorption coefficients as below (Poulin et al., 2014):

$$\alpha_{254} = Abs_{254}/L, \tag{1}$$

where, α_{254} is the decadic absorption coefficient (m^{-1}), Abs_{254} is the absorbance at 254 nm, and L represents the path length (m). Specific UV absorbance at 254 nm (SUVA$_{254}$; reported in units of $L\,mg\,C^{-1}\,m^{-1}$) was determined according to Weishaar et al. (2003):

$$SUVA_{254} = \alpha_{254}/DOC. \tag{2}$$

DOM fluorescence was determined with a fluorescence spectrophotometer (F-7000, Hitachi, Japan) to quantify humic-like, fulvic-like, and protein-like fluorescence (Fellman et al., 2010). The fate of humic-like fluorescence may be self-assembly particles or be adsorbed onto minerals, while protein-like fluorescence is tightly associated with biological processes and biodegraded into inorganic matter (Fellman et al., 2010; He et al., 2016). The excitation wavelengths ranged from 220 to 400 nm at 5 nm increments, and the emission wavelength from 280 to 500 nm at 2 nm increments. Blanks were measured daily with the same settings to correct excitation–emission matrices (EEMs). Parallel factor analysis (PARAFAC) was performed using the N-way toolbox in MATLAB (MathWorks, USA) to determine peaks (Andersson and Bro, 2000; Mostofa et al., 2019; Stedmon and Bro, 2008). Detailed procedures and criteria for applying and validating the PARAFAC model are available in Yi et al. (2021).

The PARAFAC model components identified were further compared with relevant published and reported fluorophores in the OpenFluor database (Table 1; Murphy et al., 2014). Several common indices of DOM composition were determined from EEMs, including fluorescence index (FI; McKnight et al., 2001), humification index (HIX; Ohno, 2002), and freshness index (β/α; Parlanti et al., 2000; Table 2).

2.4 Statistical analysis

The normality of the data was first examined by a Shapiro–Wilk test using SPSS 26. Normally distributed data were analyzed by one-way ANOVA with Tukey's post-test for multiple comparisons. Nonparametric data with three or more comparisons were analyzed with a Kruskal–Wallis test followed by Holm's step-down Bonferroni correction. The Mann–Whitney U test was used for comparison of distributions between two groups. The correlations among DOC concentrations, DOM properties, carbon isotopes, ion concentrations, and catchment characteristics (i.e., mean catchment slope, the proportion of different types of land use, mean annual air temperature, and mean drainage elevation) were computed by Pearson's correlation coefficient (R) using OriginPro 2021 (student version). Values are presented as the mean $\pm$ standard deviation (SD). All statistical tests were performed at a 0.05 significance level. In addition, all the statistical analyses were performed again after data from site Y12 were removed to test for possible skewing of the findings, as the sample was significantly affected by rainfall events. If not mentioned otherwise, the results from site Y12 did not skew the findings at the significance level of 0.05.

We performed a stepwise multiple linear regression (MLR) modeling to identify significant environmental factors of DOC concentrations and DOM properties using SPSS 26. All environmental factors were included in the models except for SOC because we aim to examine the impacts of human activities and geomorphology rather than the direct influence of SOC on DOC concentrations and DOM properties. The objective model with the highest adjusted R^2 value was used to infer the DOC concentrations and DOM properties. In addition to the MLR and Pearson correlation analyses to explore the relationships between environmental factors and DOC, we further used the partial least squares path model (PLS-PM) to infer direct and indirect effects of multiple factors (e.g., geomorphologic and anthropogenic impacts) on DOC concentrations and DOM properties. The PLS-PM analysis was performed using the R package "plspm" (Sanchez, 2013). Because PLS-PM offers the advantage of not imposing any distributional assumptions on the data, which enhances its broad applicability (Sanchez, 2013) and allows for the exploration of complex cause–effect relationships involving latent variables, it is a suitable technique for multivariate analyses. Each latent variable consists of one or more manifest variables (e.g., geomorphology, including elevation and slope). The environmental factors used

Table 1. Description of the three components identified by PARAFAC and comparison with previous studies from the OpenFluor database with a minimum similarity score of 0.95 (Murphy et al., 2014).

Component	Ex_{max} (nm)	Em_{max} (nm)	Description and likely structure	Number of matches in OpenFluor	Previous studies
C1	295	402	Similar to traditionally defined peak M, marine humic-like components, are products from microbial processes or autochthonous production.	6	C6 (Walker et al., 2009); C4 (Kim et al., 2022); C4 (Li et al., 2016)
C2	275	338	Protein-like (tryptophan-like) components, commonly found in anthropogenically affected rivers, are associated with recent biological production and breakdown products of lignin.	30	C3 (DeFrancesco and Guéguen, 2021); C7 (Lambert et al., 2017); C2 (Du et al., 2019)
C3	325	440	Traditional fulvic-like peaks A and C, humic-like and terrestrial delivered OM, autochthonous, or microbial source.	70	C1 (Amaral et al., 2016); C1 (Ryan et al., 2022); C1 (Shutova et al., 2014)

Table 2. DOM optical parameters used in this study.

Index name	Calculation	Description	Reference
SUVA$_{254}$	SUVA$_{254}$ = α_{254}/DOC concentration. α_{254} is the decadic UV absorbance at 254 nm.	An indicator for the degree of aromaticity. It is positively correlated with aromaticity.	Weishaar et al. (2003)
Fluorescence index (FI)	FI = Em450/Em500, at Ex 370 nm.	A proxy for DOM source. Higher values (~ 1.9) are associated with microbial sources, and lower values (~ 1.4) correlated with terrestrial sources.	McKnight et al. (2001)
Humification index (HIX)	HIX = $\sum 435$–$480/(\sum 300$–$345 + \sum 435$–$480)$, at Ex 254 nm.	Indicator of humification status of DOM. Higher HIX values indicate an increasing degree of humification.	Ohno (2002)
Freshness index (β/α)	β/α = Em380(β)/ the Em intensity maximum between 420 and 435 nm at Ex 310 nm (α).	Higher β/α values are commonly associated with the increasing contribution of recently microbially produced DOM.	Parlanti et al. (2000)

in the model were categorized into seven latent variables, including geomorphology (elevation and slope), anthropogenic activities (e.g., urban and agricultural land uses and anthropogenically derived Cl$^-$; Cl$^-_{anthro}$, calculated as the total Cl$^-$ concentration minus atmospheric contributed Cl$^-$ concentration, which is the lowest Cl$^-$ concentration at site Y5 in the Yinjiang River; Gaillardet et al., 1997; Meybeck, 1983), climate (T_{air}), SOC (SOC content), water chemistry (pH), POC (POC concentrations), and nutrient (NH$_4^+$-N and TN). The environmental factors and their manifest variables included in the model were the most critical variables identified based on the Pearson correlation results. These variables were selected after reducing the full models (initial models with more variables) to meet the requirements of the PLS-PM analysis (Du et al., 2023; Sanchez, 2013; Tian et al., 2019). In addition, the structure of the model was simplified to focus on the major effect of environmental factors

on DOC concentrations rather than to explore the effects on other factors (e.g., the geomorphologic controls on POC were ignored). The significance of the path coefficients was determined through a nonparametric bootstrap resampling of 1000 times.

3 Results

3.1 Spatial variations in water chemistry, DOC concentrations, and isotopes of DOC

Both river water and spring water were mildly alkaline with pH varying from 7.2 to 8.9, and the pH in the Yinjiang and Shiqian rivers was higher than that in the spring water (Fig. 2a). The Cl$^-$ concentration showed an increasing trend in the Yinjiang, Shiqian, and Yuqing rivers, with an average of 2.56 ± 1.03, 3.76 ± 0.83, and
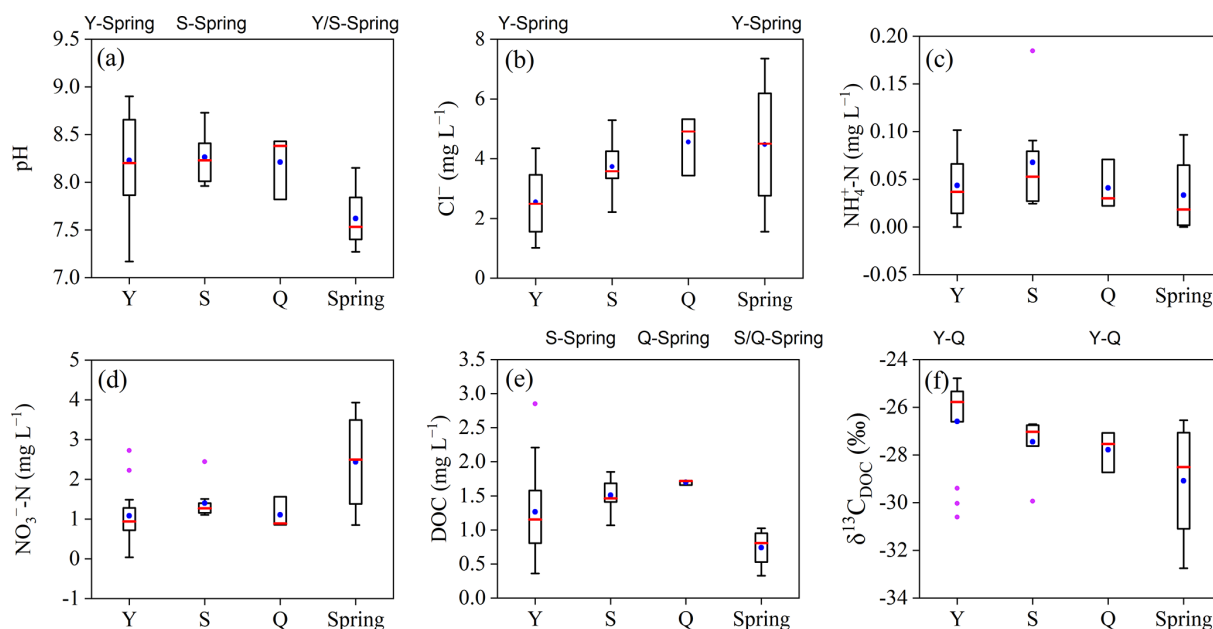
Figure 2. Spatial variations in water chemistry in the Yinjiang (Y), Shiqian (S), and Yuqing (Q) rivers and springs. **(a)** pH, **(b)** Cl^-, **(c)** NH_4^+-N, **(d)** NO_3^--N, **(e)** DOC, and **(f)** $\delta^{13}C_{DOC}$. In each box plot, the end of the box represents the 25th and 75th percentiles, the solid blue dot represents the mean, the horizontal line inside the box represents the median, and the whiskers represent 1.5 times the upper and lower interquartile ranges (IQR). The solid magenta dot represents the outlier (data points outside of the 1.5 interquartile ranges). Letters above the boxes represent significant differences between the grouping of river and/or spring water based on statistical analyses at the significance level of 0.05 (e.g., Y-Spring above panel **(b)** indicates that the Cl^- in the river water of the Yinjiang River was significantly different from that in the spring water).

$4.55 \pm 0.81 \, \text{mg L}^{-1}$, respectively (Fig. 2b). In addition, the Cl^- concentration in the spring water ($4.48 \pm 2.08 \, \text{mg L}^{-1}$) was significantly higher than that in the Yinjiang River ($p < 0.05$; Fig. 2b). In the rivers and springs, the water displayed similar NH_4^+-N concentrations with a mean value of 0.04 ± 0.03, 0.07 ± 0.05, 0.04 ± 0.03, and $0.03 \pm 0.04 \, \text{mg L}^{-1}$ in the Yinjiang, Shiqian, Yuqing rivers, and spring water (Fig. 2c). In springs, the average NO_3^--N concentration was $1.93 \pm 0.93 \, \text{mg L}^{-1}$, higher than the average in the three rivers ($1.15 \pm 0.36 \, \text{mg L}^{-1}$), although there were no significant differences for the overall NO_3^--N concentration between the rivers and springs ($p > 0.05$; Fig. 2d).

DOC concentrations in the three study rivers varied from 0.36 to $2.85 \, \text{mg L}^{-1}$, with the highest mean concentration in the Yuqing River ($1.70 \pm 0.04 \, \text{mg L}^{-1}$; Fig. 2e), followed by the Shiqian River ($1.51 \pm 0.22 \, \text{mg L}^{-1}$) and the Yinjiang River ($1.27 \pm 0.66 \, \text{mg L}^{-1}$). The DOC concentrations in spring water were significantly lower than those in the surface water of the Shiqian and Yuqing rivers ($p < 0.05$; Fig. 2e), and the average DOC concentration in spring water ($0.74 \pm 0.30 \, \text{mg L}^{-1}$) was also lower than the average DOC concentration in the Yinjiang River, indicating there must be other sources of DOC besides groundwater.

For $\delta^{13}C_{DOC}$, although the average $\delta^{13}C_{DOC}$ values showed a decreasing trend in the Yinjiang River, Shiqian River, Yuqing River, and springs, averaging

Table 3. $\Delta^{14}C_{DOC}$ and age of DOC in the Yinjiang River.

River	Samples	$\Delta^{14}C_{DOC}$ (‰)	DOC-Age (yr BP)	SD of DOC-Age (yr BP)
Yinjiang River	Y1	−92	774	25
	Y2	−74	616	23
	Y3	−52	430	27
	Y5	−40	326	27
	Y9	−59	491	27
	Y11	−51	417	27
	Y12	33	Modern	28
	Y13	−49	401	24
	Y14	−109	928	28

at $-26.6 \pm 1.8\,‰$, $-27.5 \pm 1.1\,‰$, $-27.8 \pm 0.9\,‰$, and $-29.1 \pm 2.7\,‰$, respectively, there were no statistically significant differences in the overall $\delta^{13}C_{DOC}$ values between the three rivers and springs ($p > 0.05$; Fig. 2f). The $\Delta^{14}C_{DOC}$ of the Yinjiang River varied widely from $-109\,‰$ to $33\,‰$ with an average of $-54.7 \pm 39.9\,‰$ (Table 3). The radiocarbon ages of the DOC ranged from 928 years BP (i.e., before present) to the present, and the youngest $\Delta^{14}C_{DOC}$ ($33.3\,‰$) was found at site Y12.
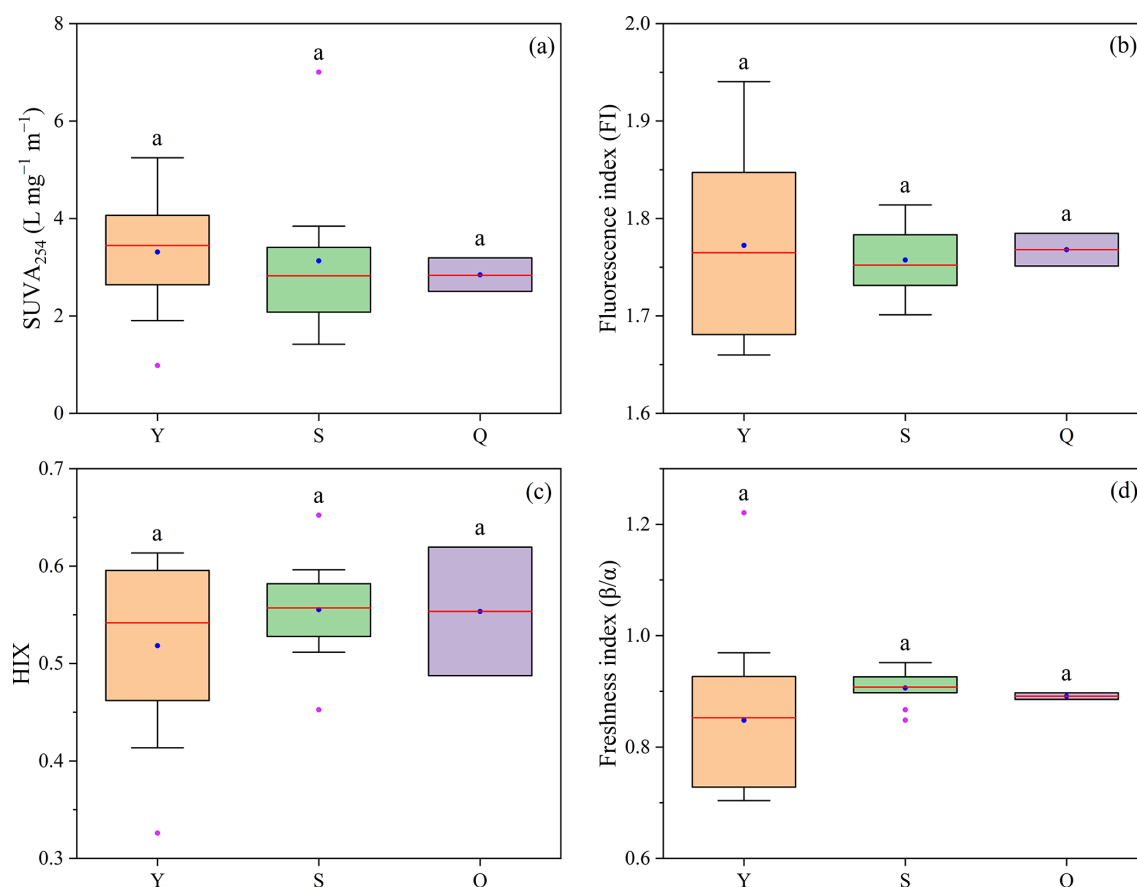
Figure 3. Spatial variations in DOM property in the Yinjiang (Y), Shiqian (S), and Yuqing (Q) catchments. **(a)** SUVA$_{254}$, **(b)** fluorescence index (FI), **(c)** HIX, and **(d)** freshness index (β/α). In each box plot, the end of the box represents the 25th and 75th percentiles, the solid blue dot represents the average, the horizontal red line represents the median, and the whiskers represent 1.5 IQR. The solid magenta dot represents the outlier, which is outside of the 1.5 interquartile range. Different lowercase letters above the boxes denote significant differences across rivers based on statistical analysis with $p < 0.05$.

3.2 Riverine DOM optical properties

Two humic-like components (C1 and C3) and one protein-like component (C2) were identified by the PARAFAC model in these three rivers (Fig. S3 in the Supplement; Table 1). Component C1 is similar to traditionally defined peak M and sourced from microbial processes or autochthonous production (Kim et al., 2022; Li et al., 2016; Walker et al., 2009). Component C2 was previously related to recent biological production (DeFrancesco and Guéguen, 2021; Du et al., 2019; Lambert et al., 2017). C3 was the most widely found component in previous research among three fluorescent components and was identified as traditional fulvic-like peaks A and C, representing terrestrial delivered OM or autochthonous microbial-sourced OM (Amaral et al., 2016; Ryan et al., 2022; Shutova et al., 2014). Although C1 and C2 varied more widely in the Yinjiang River compared with the Shiqian and Yuqing rivers, the two fluorescent components did not show a statistical difference among the three rivers ($p > 0.05$; Fig. S3a and b). However, a greater proportion

of C3 was found in the Shiqian River, exhibiting a distinctive signature compared with the Yinjiang River (Fig. S3c). The proportion of C3 did not show any significant differences between the Yuqing River and the other two rivers (i.e., the Yinjiang and Shiqian rivers).

The average SUVA$_{254}$ values were 3.3 ± 1.1, 3.1 ± 1.8, and $2.8 \pm 0.3 \, \text{L mg}^{-1} \, \text{m}^{-1}$ in the Yinjiang, Shiqian, and Yuqing rivers, respectively, without significant spatial differences across the three rivers ($p > 0.05$; Fig. 3a). For the FIs, the overall fluorescence property did not vary significantly among the three rivers ($p > 0.05$; Fig. 3b–d). FI varied in a narrow range compared with β/α and HIX. The FI of DOM ranged from 1.66 to 1.94, averaging 1.78 (Fig. 3b), indicating a mixture of DOM of terrestrial and microbial origins. By comparison, β/α varied from 0.70 to 1.22 (Fig. 3d), and HIX varied from 0.33 to 0.65 (Fig. 3c), with greater variability among the three rivers.
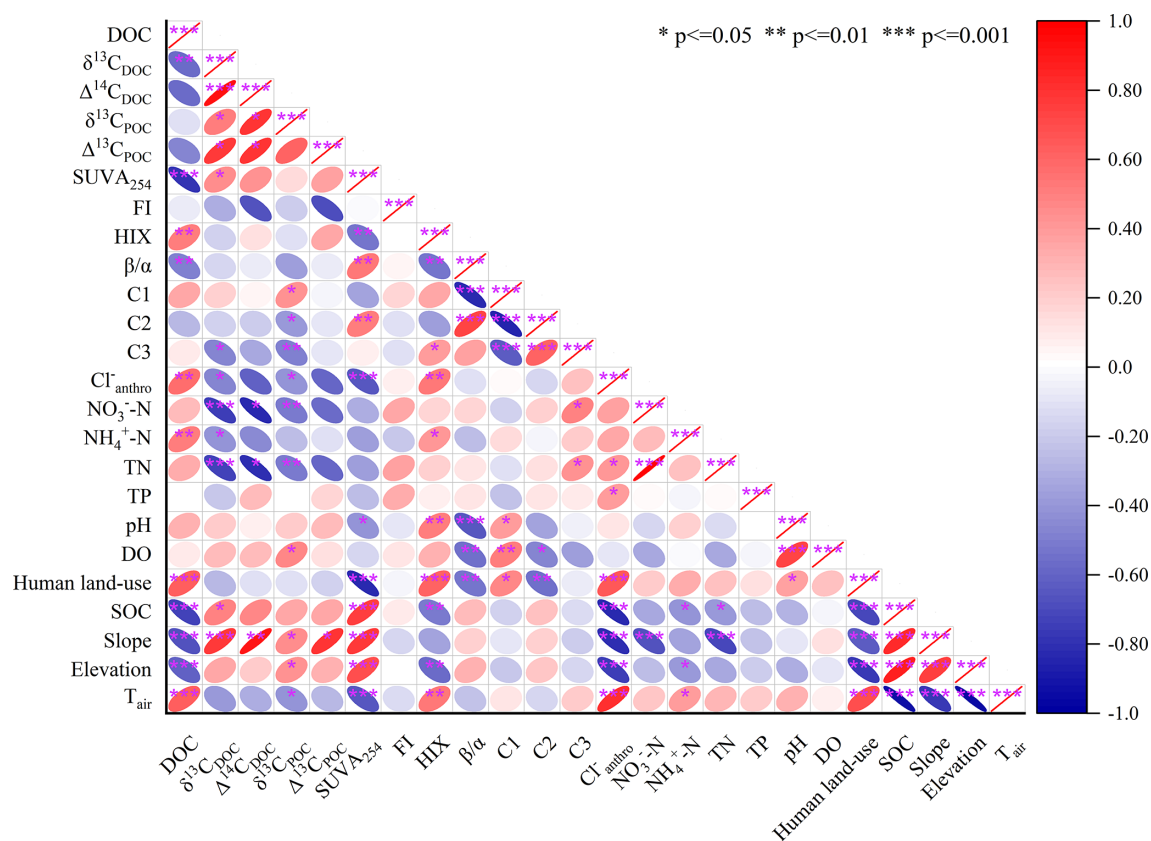
Figure 4. Correlation plot of the selected water chemistry and catchment characteristics. The colors represent the degree of pairwise correlation regarding Pearson's correlation coefficient. $\delta^{13}C_{DOC}$ and $\Delta^{14}C_{DOC}$ at site Y12 were excluded from the analysis as the sample was collected after a rainfall event. In addition, $SUVA_{254}$ at site S3 was excluded from the analysis as the sample was strongly influenced by road construction, which was evidenced by high POC and TSM concentrations (Chen et al., 2021). Human land use denotes the proportion of urban and agricultural land use. Elevation and T_{air} represent mean drainage elevation and annual air temperature, respectively.

3.3 Factors influencing DOC concentrations, isotopes of DOC, and DOM optical properties

Significant pairwise interdependencies between DOC and catchment characteristics were identified in the three study rivers (Fig. 4). There is a strong negative correlation between DOC and SOC ($p < 0.001$, $r = -0.73$; Fig. 4), as well as average catchment slope ($p < 0.001$, $r = -0.67$). Conversely, DOC displayed a positive correlation with the proportion of urban and agricultural land uses ($p < 0.001$, $r = 0.62$), Cl^-_{anthro} ($p < 0.01$, $r = 0.58$), and NH_4^+-N ($p < 0.01$, $r = 0.51$). Stepwise MLR models revealed that topsoil SOC and POC were the most effective predictors for explaining the spatial variation in DOC concentrations (Table 4), while catchment slope and NH_4^+-N exhibited the highest explanatory power for DOC concentrations when SOC was excluded from the models. Unlike DOC, a significant positive correlation with mean catchment slope was found for $\delta^{13}C_{DOC}$ ($p < 0.001$, $r = 0.76$; Fig. 4). In addition, there was a significant negative correlation between $\delta^{13}C_{DOC}$ and NO_3^--N ($p < 0.001$, $r = -0.75$). More-

over, $\delta^{13}C_{DOC}$ was negatively correlated with DOC concentrations ($p < 0.01$, $r = -0.57$; Fig. 4), but positively correlated with $\delta^{13}C_{POC}$ in these three rivers ($p < 0.05$, $r = 0.51$). Similar to $\delta^{13}C_{DOC}$, $\Delta^{14}C_{DOC}$ was positively related to mean catchment slope ($p < 0.01$, $r = 0.91$) and $\Delta^{14}C_{POC}$ ($p < 0.05$, $r = 0.79$). Additionally, there was a positive correlation between $\Delta^{14}C_{POC}$ and catchment slope ($p < 0.05$, $r = 0.79$), and no significant correlations were detected between $\Delta^{14}C_{POC}$ and the proportion of urban and agricultural land uses or ions that reflect human disturbances (e.g., Cl^-_{anthro}, NH_4^+-N, and NO_3^--N; $p > 0.05$; Fig. 4).

$SUVA_{254}$ showed an increasing trend with increasing mean catchment slope ($p < 0.001$, $r = 0.77$; Fig. 4). Furthermore, there was a significant negative correlation between $SUVA_{254}$ and the proportion of urban and agricultural land uses ($p < 0.001$, $r = -0.83$). This is consistent with the constructed stepwise MLR models that urban and agricultural land uses and catchment slope were the best predictors of $SUVA_{254}$ (Table 4). Although no significant correlation was observed between the FIs and catchment slope, they (except for FI) were found to be closely related to land use pat-

Table 4. Multiple stepwise linear regression models of catchment attributes and water chemistry for DOC concentrations and DOM properties.

Dependent variables	Predictors	Model equation	n	Adj. R^2	Significance level
DOC*	Slope, NH_4^+-N	$= -0.109 \cdot \text{slope} + 4.295 \cdot NH_4^+ - N + 3.375$	28	0.50	$p < 0.001$
DOC	SOC, POC	$= -0.006 \cdot \text{SOC} + 0.384 \cdot \text{POC} + 4.145$	28	0.59	$p < 0.001$
SUVA$_{254}$	Urban and agricultural land use, slope	$= -5.461 * \text{urban and agricultural land use} + 0.145 \cdot \text{slope} + 1.318$	26	0.77	$p < 0.001$
HIX	Urban and agricultural land use	$= 0.433 \cdot \text{urban and agricultural land use} + 0.438$	27	0.34	$p < 0.001$
FI		No variables were entered into the equation.	27		
β/α	pH	$= -0.195 \cdot \text{pH} + 2.476$	27	0.41	$p < 0.001$
C1	DO, TP, urban and agricultural land use	$= 7.713 \cdot \text{DO} - 220.846 \cdot \text{TP} + 90.905 \cdot \text{urban and agricultural land use} - 36.005$	27	0.46	$p < 0.001$
C2	Urban and agricultural land use, DO	$= -48.748 \cdot \text{urban and agricultural land use} - 2.515 \cdot \text{DO} + 58.255$	27	0.36	$p = 0.002$
C3	NO_3^--N, POC	$= 4.181 \cdot NO_3^-\text{-N} + 3.738 \cdot \text{POC} + 3.826$	27	0.34	$p = 0.003$

* SOC was not included as predictor in this model so as to examine the impacts of human activities and geomorphology, rather than the direct influence of SOC on DOC concentrations.

terns (Fig. 4). For example, HIX had a positive correlation with urban and agricultural land uses ($p < 0.001$, $r = 0.61$; Fig. 4), while β/α had a negative correlation with urban and agricultural land uses ($p < 0.01$, $r = -0.52$) and water pH ($p < 0.001$, $r = -0.66$). In addition, the fluorescent components did not exhibit significant variations with changing catchment slope ($p > 0.05$; Fig. 4), but the percentage of C1 and C2 were positively ($p < 0.05$, $r = 0.47$) or negatively ($p < 0.01$, $r = -0.55$) related to the proportion of urban and agricultural land uses. Urban and agricultural land uses were also identified as predictors for DOM optical indexes (i.e., HIX; Table 4) and fluorescent components (i.e., C1 and C2). However, unlike C1 and C2, C3 was not significantly correlated with urban and agricultural land uses ($p > 0.05$; Fig. 4), but its variation can be partially explained by NO_3^--N concentrations and POC (Table 4).

3.4 Direct and indirect effects of environmental factors on DOC concentrations

The PLS-PM analysis showed that 67 % of the variance in DOC concentrations could be explained by our seven environmental factors constructed ($R^2 = 0.67$, Fig. 5a). The total effect on DOC concentrations is strongest from geomorphology (-0.65), followed by SOC (-0.45), anthropogenic activities (0.39), climate (0.38), POC (0.27), nutrients (0.21), and water chemistry (0.10) (Fig. 5b). The results indicated that geomorphology was the most significant factor in controlling DOC concentrations, primarily through indirect regulation of SOC content, which was directly influenced by annual catchment temperature and anthropogenic activities (Fig. 5a and b). By comparison, anthropogenic activities not only indirectly regulated riverine DOC concentrations through SOC, but also had a significant indirect impact on DOC concentrations through the regulation of nutrient levels. Similar to DOC concentrations, geomorphology (-0.53) exhibited the most pronounced effects on fluorescent components (Fig. S4 in the Supplement). However, anthropogenic activities (0.49) demonstrated a comparable effect on fluorescent components, primarily through a direct pathway (0.37; Fig. S4b). Anthropogenic activities (-0.84) were the strongest driver for DOM optical parameters, although geomorphology (0.59) played a significant role in indirectly influencing DOM optical parameters (Fig. S5 in the Supplement).

4 Discussion

4.1 Geomorphologic controls on DOC export

Catchment slope, which is often closely associated with catchment elevation (Fig. 4), is an important predictor of DOC concentrations because catchment slope is a key factor in affecting flow velocity and thus water retention time (Harms et al., 2016; Mzobe et al., 2020). The negative relationship between DOC and SOC (Fig. 4 and Table 4) and the positive correlation between slope and $\Delta^{14}C_{POC}$ or $\Delta^{14}C_{DOC}$ are consistent with previous findings that a shorter water retention time in high-relief regions can reduce DOC export from SOC stocks and mobilize organic carbon
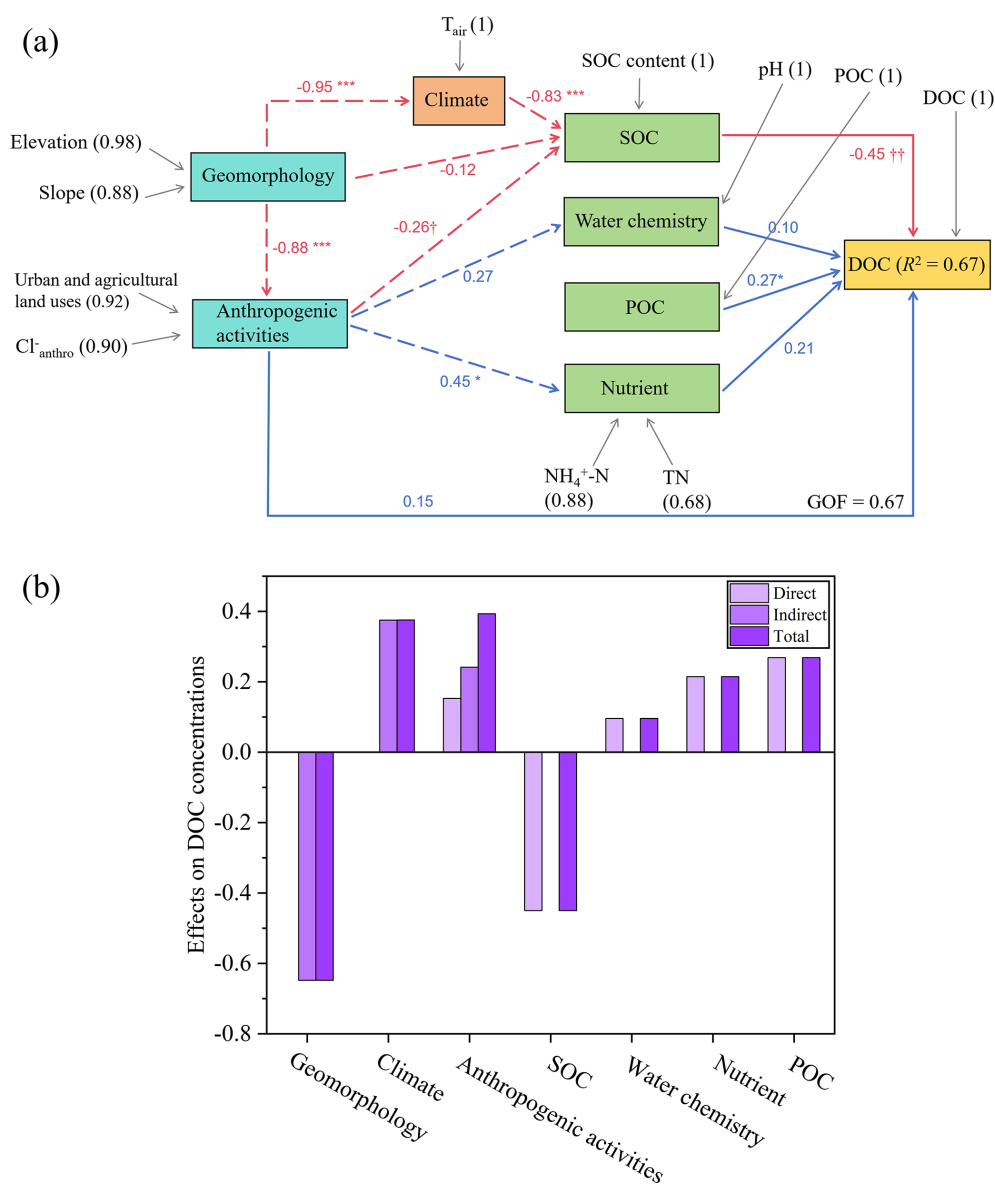
Figure 5. The most parsimonious PLS-PM model shows the direct and indirect effects of geomorphology and anthropogenic activities on DOC concentrations. **(a)** Path coefficients are shown as arrows with blue and red to represent positive and negative effects, respectively. The solid and dotted lines indicate the direct and indirect influence pathways of environmental drivers on DOC concentrations, respectively. The indicators (e.g., TN) of latent variables (e.g., nutrient) are shown at the beginning of the gray arrows. The numbers in the parentheses are the loading scores. GOF denotes the goodness of fit of the entire model. R^2 indicates the amount of variance in DOC concentrations explained by its independent latent variables. The standardized path coefficients that are significantly different from zero are indicated by * $p \leq 0.05$, ** $p \leq 0.01$, *** $p \leq 0.001$, † $p = 0.06$, †† $p = 0.07$. **(b)** Standardized direct and indirect mean effects of environmental drivers on DOC concentrations derived from the PLS-PM analysis.

with younger ages (Catalán et al., 2016). The decreasing organic carbon export in catchments with higher slopes partially explains why high-relief regions exhibit lower riverine DOC concentrations despite having a higher SOC content. Compared with high-relief regions, low-relief regions would discharge more aged organic carbon into rivers when relatively ^{14}C-depleted DIC and CO_2 (aq) derived from carbonate weathering are incorporated into primary production

in low-relief regions, as also evidenced by the positive relationship between the slope and $\Delta^{14}C_{POC}$ (Fig. 4). Furthermore, the aged riverine DOC has also been attributed to the input of deeper, older soil organic matter through deeper flow paths (Barnes et al., 2018; Masiello and Druffel, 2001). This aged DOC, discharged through deeper water flow paths, may have also served as an important source of DOC in low-relief regions of this study. The correlation of $SUVA_{254}$ with the

mean catchment slope suggests that steeper catchments tend to export DOC with more aromaticity (Fig. 4 and Table 4), indicating the geomorphologic effects on DOM characteristics. Previous research has reported that the aromatic content of DOM tends to decline if DOM is derived from deeper soil profiles (Inamdar et al., 2011), which is attributed to the sorption of aromatic DOM when subsurface flow water percolates through the soil profile.

Microbial degradation has been well recognized as a critical factor in controlling organic material preservation in soils (Barnes et al., 2018). Previous studies have reported a decreasing $\delta^{13}C_{DOC}$ with increasing DOC concentrations in spring water (Nkoue Ndondo et al., 2020) and for TOC in soil profiles (Lloret et al., 2016; Nkoue Ndondo et al., 2020). We observed a comparable relationship in river water of the three catchments (Fig. 4). This can be explained by the lateral transport of DOC from microbially active soil horizons into rivers (Lambert et al., 2011), resulting in the enhanced biodegradation of DOC with the preferential removal of ^{12}C. As a result, the remaining DOC with lower concentrations is typically characterized by a heavier $\delta^{13}C_{DOC}$ (Nkoue Ndondo et al., 2020; Opsahl and Zepp, 2001), which further indicates that the low-concentration DOC in the three rivers is the result of substantial microbial degradation.

Groundwater with significant SOC inputs due to highly active microbial activities has long been recognized as a substantial source of DOC (McDonough et al., 2020; Shen et al., 2015). Several studies have reported increased groundwater contributions with distance downstream at the watershed scale (Cowie et al., 2017; Iwasaki et al., 2021). The strong positive relationship between conductivity and $\delta^{18}O$ ($p < 0.001$; Fig. S6a in the Supplement) is primarily due to the mixing of two end-members (i.e., high-conductivity with ^{18}O-enriched groundwater and low-conductivity with $\delta^{18}O$-depleted headstream water) for river water (Lambs, 2004), although it may also indicate the impact of evaporation in the catchment (Zhong et al., 2020). In addition, the $\delta^{18}O$ values increased progressively from upstream to downstream (Fig. S6b), which also validates the two sources (i.e., headstream water and groundwater) of downstream river water, indicating that groundwater was most likely an essential contributor to downstream river water. This also supports our earlier hypothesis that aged DOC could be exported into rivers through deeper water flow paths. However, groundwater was probably not the primary source of riverine DOC due to the relatively low groundwater DOC concentrations as compared with riverine DOC concentrations (Fig. 2e; groundwater is shown as "spring"). Moreover, the groundwater contribution was probably much less significant in the wet season (e.g., September in the study area), even in catchments where DOC is mainly derived from groundwater (Lloret et al., 2016). Thus, we infer groundwater is an important but not a primary source of riverine DOC in the three study rivers.

4.2 Anthropogenic impacts on DOC

Previous research has found significant changes in DOC concentrations and DOM composition in agricultural and urban landscapes (Spencer et al., 2019; Stanley et al., 2012). Conversion of native forest and pasture to row crop agriculture may lead to substantial losses of SOC stores due to greatly accelerated erosion and decomposition rates (Guo and Gifford, 2002; Montgomery, 2007; Stanley et al., 2012). By comparison, natural vegetation could greatly reduce SOC input into rivers by effectively reducing soil erosion through the consolidation effect of roots on soil and the interception of rainfall by stems and leaves (Zhang et al., 2019). Agricultural activities tend to liberate SOC through erosion over longer timescales and cause an elevated DOC export into rivers (Figs. 4 and 5), although DOC of urban origin can also make a massive contribution to the riverine DOC pool (Sickman et al., 2007). Yet, anthropogenic impacts can also result in decreased DOC concentrations globally due to reduced organic carbon inputs into soils and enhanced SOC decomposition induced by warmer temperatures (Nagy et al., 2018; Spencer et al., 2019) or lead to undetectable changes in DOC concentrations (Veum et al., 2009). These different responses are mainly due to diverse farming practices and the associated changing effects on terrestrial and aquatic carbon dynamics (Stanley et al., 2012).

Anthropogenic activities are important factors for the pervasive increase in nutrient and ion concentrations (Chetelat et al., 2008; Smith and Schindler, 2009). For catchments without evaporite outcrops, their riverine Cl^- excluding atmospheric contribution can be regarded as mainly of anthropogenic origin (Cl^-_{anthro}), which is a strong indicator of anthropogenic activities (Fig. 5). The positive relationship between DOC concentrations and Cl^-_{anthro}, as shown in Fig. 4, also demonstrated anthropogenic impacts on DOC export. Nutrient enrichment has been a well-known contributor to eutrophication (Paerl, 2009). In conjunction with increasing water residence time due to damming (Fig. 1a), our results demonstrate that increased nutrient inputs into rivers will enhance algae production (Chen et al., 2021) and, eventually, accumulation of DOC (as evidenced by the relationship between NH_4^+-N and DOC in Fig. 4 with NH_4^+-N serving as a predictor for DOC; see Table 4). A recent study conducted in the Longtan Reservoir in the Xijiang River basin in southwest China with widespread karst landscape (similar to our study area) found that a majority of its POC was intercepted or degraded within the reservoir, with the POC primarily originating from phytoplankton (Yi et al., 2022). Its carbon isotope composition of POC ($\delta^{13}C_{POC}$) ranged from $-35‰$ to $-30‰$, which is relatively depleted, and the POC was found to be a significant contributor to the reservoir DOC (Yi et al., 2022). Thus, the lower $\delta^{13}C_{DOC}$ with increasing NO_3^--N further indicated the greater algae- or C3 plant-derived DOC accumulation with a higher level of nutrients (Fig. 4 and Table 4).

Despite the fact that anthropogenic impacts on DOM characteristics and age have been widely proposed in the past two decades (Butman et al., 2014; Coble et al., 2022; Zhou et al., 2021), there are no clear relationships between land use and ^{14}C ages in our study area, which may result from large variations in soil characteristics and limited ^{14}C data. However, DOM characteristics were found to be closely related to land use patterns (Figs. S4 and S5; Table 4). Although significant relationships with urban and agricultural land uses were found for C1 and C2 (Fig. 4; Table 4), it remains unclear how the autochthonous contribution to the riverine DOC pool varied with land use change because C1 and C2 are both probably derived from autochthonous production but exhibit opposing trends with increasing urban and agricultural land uses (Table 1). Overall, DOM in catchments with a higher proportion of urban and agricultural land uses was distinct from other catchments as it was less aromatic (SUVA$_{254}$, Fig. 4), less recently produced (β/α), and had a higher degree of humification (HIX). SUVA$_{254}$ values for the three study rivers were comparable with those reported in coastal glacier mountainous streams with late succession in southeast Alaska ($3.4 \pm 0.5\,L\,mg^{-1}\,m^{-1}$, $n = 5$; Holt et al. 2021) and in the anthropogenic-influenced downstream of the Yangtze River ($3.4 \pm 1.1\,L\,mg^{-1}\,m^{-1}$, $n = 82$; Zhou et al. 2021). Lower DOM aromaticity in the urban and agricultural streams and rivers was consistent with previous studies (Hosen et al., 2014; Kadjeski et al., 2020), which suggested a microbial origin for the DOM. However, it is important to note that this phenomenon was not universally observed (Zhou et al., 2021). Furthermore, the less aromatic and less recently produced DOM could be due to soil organic materials from deep soil profiles as a result of increased soil erosion by anthropogenic activities (Inamdar et al., 2011; Stanley et al., 2012).

4.3 Biogeochemical processes of DOC and comparison of Δ^{14}C$_{DOC}$ in mountainous rivers

In this study, geomorphologic characteristics and anthropogenic activities were identified as significant drivers of DOC export and DOM composition across broad spatial scales. Here, we further examine how these two factors regulate the biogeochemical processes of DOC. As discussed earlier, both geomorphology and anthropogenic activities are significant factors controlling DOC concentrations. The PLS-PM analysis further revealed that the combined effects of the two factors on DOC were mainly achieved through indirect influences on SOC content (Fig. 5). In contrast to the direct impact of anthropogenic activities on SOC through soil erosion, the controls exerted by geomorphology on SOC were closely linked to climate. Lower altitudes are typically associated with higher annual air temperatures (Fig. 4), which promote terrestrial net primary production and the microbial degradation of SOC (Voss et al., 2015), resulting in the accumulation of large quantities of DOC in soils (Creed

et al., 2018). Geomorphology is also associated with reduced water retention time due to rapid flows, leading to a lower input of terrestrially derived DOC into rivers, as discussed earlier. It is worth noting that the conversion of POC to DOC through dissolution and desorption (He et al., 2016) is also an important source of riverine DOC (Fig. 5). Contrary to DOC concentrations, although the percentage of urban and agricultural land uses was significantly correlated with mean catchment slope (Fig. S1d), anthropogenic activities were identified as more effective predictors for DOM characteristics than geomorphology (Table 4), highlighting the crucial role of anthropogenic activities in regulating DOM dynamics. Therefore, the biogeochemical processes of DOM in the three rivers studied here were collectively affected by geomorphologic controls and anthropogenic impacts. In particular, geomorphologic controls on DOM were mainly evidenced by carbon isotopes, while anthropogenic impacts were primarily supported by the DOM fluorescence characteristics (Fig. 4 and Table 4). There was no significant relationship between carbon isotopes and optical properties, which is inconsistent with previous studies (Aiken et al., 2014; Butman et al., 2012; Zhou et al., 2018). This discrepancy is most likely due to the potential masking effect of autochthonous DOM, as also evidenced by the decoupled relationship between Δ^{14}C$_{DOC}$ and SUVA$_{254}$ in the St. Lawrence River (Aiken et al., 2014; Butman et al., 2012). Disentangling the dual influences (geomorphologic and anthropogenic) is challenging because they have collectively affected both DOC concentration and DOM quality in these rivers. A comprehensive assessment of the biogeochemical processes of DOC and their multiple controlling factors will advance our understanding of riverine carbon cycling.

To provide deeper insight into the DOC characteristics of the study rivers, DOC concentrations and the carbon isotopes of DOC in global mountainous rivers are compiled and shown in Table 5. Δ^{14}C$_{DOC}$ in the Yinjiang River ($-54.7 \pm 39.9\,‰$; Tables 3 and 5) is lower than that of the global average ($-11.5 \pm 134\,‰$; Marwick et al., 2015), while it is similar to many other mountainous rivers (e.g., the Mackenzie River) and small mountainous rivers in Puerto Rico; Moyer et al., 2013). Δ^{14}C$_{DOC}$ values for the global mountainous streams and rivers were shown by climate (according to the Köppen–Geiger climate classification) (Beck et al., 2018; Table 5) and ranged from tropical monsoon climate (Marwick et al., 2015), temperate oceanic climate (Evans et al., 2007), cold semi-arid climates (Spencer et al., 2014), and continental subarctic climate (Hood et al., 2009). Fresh DOC in mountainous rivers was reported across climates (Evans et al., 2007; Mayorga et al., 2005; Voss et al., 2022). By contrast, the most aged DOC was observed in the Tibetan Plateau (Song et al., 2020; Spencer et al., 2014) and the Gulf of Alaska (Hood et al., 2009). The riverine aged DOC from these regions with cold climates was mainly sourced from melting glaciers with high bioavailability (Hood et al., 2009; Spencer et al., 2014) or derived from

Table 5. Comparison of carbon isotopes of DOC in mountainous rivers worldwide.

Rivers/region	Sampling date (mm/yyyy)	Climate	(mg L^{-1}) (mg L^{-1})	(‰) (‰)	(‰) (‰)	References
The Yinjiang River (China)	08/2018	Tropical	1.3 ± 0.7	-26.6 ± 1.9	-55 ± 38	This study
Zambezi (Mozambique)	02/2012–04/2012		2.4 ± 0.6	-21.9 ± 2.4	64 ± 23	Marwick et al., 2015
Betsiboka (Madagascar)	01/2012–02/2012		1.3 ± 0.6	-22.8 ± 2.1	86 ± 43	
Amazon[a]	05/1995–10/1996		1.9 ± 0.7	-26.0 ± 3.0	94 ± 176	Mayorga et al., 2005
Guanica and Fajardo (Puerto Rico)	09/2004–03/2008		2.3 ± 2.1	-26.1 ± 3.1	-55 ± 105	Moyer et al., 2013
North-west Australia (Australia)	05/2010 and 06/2011		1.5 ± 0.7	-25.0 ± 1.7	-67 ± 124	Fellman et al., 2014
Santa Clara (USA)	11/1997–03/1998	Temperate	6.2 ± 2.7	-26.1 ± 0.9	-148 ± 58	Masiello and Druffel, 2001
Conwy (Wales)[b]			9.2 ± 7.3	-28.0 ± 1.8	105 ± 6	Evans et al., 2007
Brocky Burn (Scotland)	02/1998 and 06/1998			-27.9 ± 0.2	29 ± 12	Palmer et al., 2001
Southeast Alaska	07/2013	Continental	0.8 ± 0.2	-27.0 ± 1.6	-93 ± 77	Holt et al., 2021
Gulf of Alaska	07/2008		1.2 ± 0.5	-23.9 ± 1.1	-207 ± 121	Hood et al., 2009
Alaska[c]	05/2012–10/2012		3.7 ± 4.1	-27.4 ± 0.8	-10 ± 55	Behnke et al., 2020
Kolyma (Russia)[d]	01/2003–12/2003			-28.5 ± 1.3	57 ± 51	Neff et al., 2006
Hudson (USA)[e]	01/2004		5.9 ± 0.7	-27.0 ± 0.0	-26 ± 13	Raymond et al., 2004
Central Ontario (Canada)	1990–1992		6.4 ± 4.5		96 ± 79	Schiff et al., 1997
Mackenzie River Basin (Canada)[f]	06/2018		4.3 ± 1.8	-26.9 ± 0.2	-55 ± 72	Campeau et al., 2020
Mulde (Germany)	08/2008–10/2010		9.8 ± 7.3	-26.6 ± 0.5	7 ± 27	Tittel et al., 2013
Fraser (Canada)	07/2009–05/2011		4.1 ± 5.6	-26.5 ± 0.5	58 ± 34	Voss et al., 2022
Yangtze River source region (China)	02/2017–12/2017		2.9 ± 1.4	-27.9 ± 3.3	-397 ± 185	Song et al., 2020
Tibetan Plateau (China)		Continental/dry	0.27 ± 0.0	-23.5 ± 0.2	-209 ± 71	Spencer et al., 2014

[a] Only rivers draining mountainous areas from the Andean Cordillera were reported. [b] Data were obtained from Marwick et al. (2015). [c] Calculated from mean values. [d] Only mountainous and upland rivers were reported. [e] Only the Upper Hudson River was reported. [f] Only tributaries sourced from Cordillera were reported.

permafrost thaws in deeper soil horizons with deeper flow paths (Song et al., 2020). As global air temperature increases, the greater input of the aged yet microbially labile DOC into rivers would lead to increasing emissions of CO_2 and CH_4, which in turn intensifies global warming (Vonk and Gustafsson, 2013).

5 Conclusions

This study provided insights into the DOC dynamics and their influencing factors in anthropogenically impacted subtropical small mountainous rivers. Variations in DOC concentrations are regulated by both geomorphologic and anthropogenic disturbances. We observed a positive relationship between DOC concentrations and anthropogenic land use but a negative correlation between DOC concentration and catchment slope. Carbon isotope variations were mainly due to changing mean catchment slope, while fluorescence properties of DOM were highly influenced by land use. Additionally, we found increased aromaticity with elevated catchment slope and reduced agricultural and urban land uses, indicating the geomorphologic and anthropogenic controls on DOM characteristics. We attribute these diverse DOC responses to altered water retention time, SOC dynamics, and water flow paths. This study highlights that the combination

of dual carbon isotopes and optical properties are valuable tools in tracing the origin of riverine DOC and its in-stream processes. With continued economic development and population growth, anthropogenic impacts on DOC are expected to become increasingly evident. However, anthropogenic impacts may alter various biogeochemical processes of DOC in different catchments with changing geomorphologic features due to complicated regulating mechanisms of organic carbon cycling, which to date remains poorly understood. Further studies are warranted to fully understand the combined effects of local geomorphologic controls and increasing anthropogenic impacts on DOC cycling.

Author contributions. JZ and SL conceived and designed the study. WW, JZ, and ZY contributed to the fieldwork. SC, WW, YY and

References

Aiken, G. R., Gilmour, C. C., Krabbenhoft, D. P., and Orem, W.: Dissolved organic matter in the Florida Everglades: implications for ecosystem restoration, Crit. Rev. Environ. Sci. Technol., 41, 217–248, https://doi.org/10.1080/10643389.2010.530934, 2011.

Aiken, G. R., Spencer, R. G. M., Striegl, R. G., Schuster, P. F., and Raymond, P. A.: Influences of glacier melt and permafrost thaw on the age of dissolved organic carbon in the Yukon River basin, Global Biogeochem. Cy., 28, 525–537, https://doi.org/10.1002/2013gb004764, 2014.

Amaral, V., Graeber, D., Calliari, D., and Alonso, C.: Strong linkages between DOM optical properties and main clades of aquatic bacteria, Limnol. Oceanogr., 61, 906–918, https://doi.org/10.1002/lno.10258, 2016.

Andersson, C. A. and Bro, R.: The N-way toolbox for MATLAB, Chemometr. Intell. Lab., 52, 1–4, 2000.

Ask, J., Karlsson, J., Persson, L., Ask, P., Byström, P., and Jansson, M.: Terrestrial organic matter and light penetration: Effects on bacterial and primary production in lakes, Limnol. Oceanogr., 54, 2034–2040, https://doi.org/10.4319/lo.2009.54.6.2034, 2009.

Barnes, R. T., Butman, D. E., Wilson, H. F., and Raymond, P. A.: Riverine Export of Aged Carbon Driven by Flow Path Depth and Residence Time, Environ. Sci. Technol., 52, 1028–1035, https://doi.org/10.1021/acs.est.7b04717, 2018.

Beck, H. E., Zimmermann, N. E., McVicar, T. R., Vergopolan, N., Berg, A., and Wood, E. F.: Present and future Koppen-Geiger climate classification maps at 1-km resolution, Scientific Data, 5, 180214, https://doi.org/10.1038/sdata.2018.214, 2018.

Behnke, M. I., Stubbins, A., Fellman, J. B., Hood, E., Dittmar, T., and Spencer, R. G. M.: Dissolved organic matter sources in glacierized watersheds delineated through compositional and carbon isotopic modeling, Limnol. Oceanogr., 66, 438–451, https://doi.org/10.1002/lno.11615, 2020.

Butman, D., Raymond, P. A., Butler, K., and Aiken, G.: Relationships between Delta C-14 and the molecular quality of dissolved organic carbon in rivers draining to the coast from the conterminous United States, Global Biogeochem. Cy., 26, GB4014, https://doi.org/10.1029/2012GB004361, 2012.

Butman, D. E., Wilson, H. F., Barnes, R. T., Xenopoulos, M. A., and Raymond, P. A.: Increased mobilization of aged carbon to rivers by human disturbance, Nat. Geosci., 8, 112–116, https://doi.org/10.1038/ngeo2322, 2014.

Cai, W. J.: Estuarine and coastal ocean carbon paradox: CO_2 sinks or sites of terrestrial carbon incineration?, Annu. Rev. Mar. Sci., 3, 123–145, https://doi.org/10.1146/annurev-marine-120709-142723, 2011.

Campeau, A., Soerensen, A., Martma, T., Åkerblom, S., and Zdanowicz, C.: Controls on the 14C-content of dissolved and particulate organic carbon mobilized across the Mackenzie River basin, Canada, Global Biogeochem. Cy., 34, e2020GB006671, https://doi.org/10.1029/2020gb006671, 2020.

Catalán, N., Marcé, R., Kothawala, D. N., and Tranvik, L. J.: Organic carbon decomposition rates controlled by water retention time across inland waters, Nat. Geosci., 9, 501–504, https://doi.org/10.1038/ngeo2720, 2016.

Chen, S., Zhong, J., Li, C., Wang, W.-f., Xu, S., Yan, Z.-l., and Li, S.-l.: The chemical weathering characteristics of different lithologic mixed small watersheds in Southwest China, Chinese J. Ecol., 39, 1288–1299, 2020 (in Chinese with English abstract).

Chen, S., Zhong, J., Li, S., Ran, L., Wang, W., Xu, S., Yan, Z., and Xu, S.: Multiple controls on carbon dynamics in mixed karst and non-karst mountainous rivers, Southwest China, revealed by carbon isotopes (δ^{13}C and Δ^{14}C), Sci. Total Environ., 791, 148347, https://doi.org/10.1016/j.scitotenv.2021.148347, 2021.

Chetelat, B., Liu, C.-Q., Zhao, Z., Wang, Q., Li, S., Li, J., and Wang, B.: Geochemistry of the dissolved load of the Changjiang Basin rivers: anthropogenic impacts and chemical weathering, Geochim. Cosmochim. Ac., 72, 4254–4277, 2008.

Coble, A. A., Wymore, A. S., Potter, J. D., and McDowell, W. H.: Land Use Overrides Stream Order and Season in Driving Dissolved Organic Matter Dynamics Throughout the Year in a River Network, Environ. Sci. Technol., 56, 2009–2020, https://doi.org/10.1021/acs.est.1c06305, 2022.

Connolly, C. T., Khosh, M. S., Burkart, G. A., Douglas, T. A., Holmes, R. M., Jacobson, A. D., Tank, S. E., and McClelland, J. W.: Watershed slope as a predictor of fluvial dissolved organic matter and nitrate concentrations across geographical space and catchment size in the Arctic, Environ. Res. Lett., 13, 104015, https://doi.org/10.1088/1748-9326/aae35d, 2018.

Cowie, R. M., Knowles, J. F., Dailey, K. R., Williams, M. W., Mills, T. J., and Molotch, N. P.: Sources of streamflow along a headwater catchment elevational gradient, J. Hydrol., 549, 163–178, https://doi.org/10.1016/j.jhydrol.2017.03.044, 2017.

Creed, I. F., Bergstrom, A. K., Trick, C. G., Grimm, N. B., Hessen, D. O., Karlsson, J., Kidd, K. A., Kritzberg, E., McKnight, D. M., Freeman, E. C., Senar, O. E., Andersson, A., Ask, J., Berggren, M., Cherif, M., Giesler, R., Hotchkiss, E. R., Kortelainen, P., Palta, M. M., Vrede, T., and Weyhenmeyer, G. A.: Global change-driven effects on dissolved organic matter composition: Implications for food webs of northern lakes, Global Change Biol., 24, 3692–3714, https://doi.org/10.1111/gcb.14129, 2018.

DeFrancesco, C. and Guéguen, C.: Long-term Trends in Dissolved Organic Matter Composition and Its Relation to Sea Ice in the Canada Basin, Arctic Ocean (2007–2017), J. Geophys. Res.-Oceans, 126, e2020JC016578, https://doi.org/10.1029/2020jc016578, 2021.

Devesa-Rey, R. and Barral, M. T.: Allochthonous versus autochthonous naturally occurring organic matter in the Anllóns river bed sediments (Spain), Environ. Earth Sci., 66, 773–782, https://doi.org/10.1007/s12665-011-1286-3, 2011.

Dong, K., Lang, Y., Hu, N., Zhong, J., Xu, S., Hauser, T.-M., and Gan, R.: The new AMS facility at Tianjin University, Radiation Detection Technology and Methods, 2, 1–6, https://doi.org/10.1007/s41605-018-0064-0, 2018.

Du, Y., Zhang, Q., Liu, Z., He, H., Lurling, M., Chen, M., and Zhang, Y.: Composition of dissolved organic matter controls interactions with La and Al ions: Implications for phosphorus immobilization in eutrophic lakes, Environ. Pollut., 248, 36–47, https://doi.org/10.1016/j.envpol.2019.02.002, 2019.

Du, Y., Chen, F., Zhang, Y., He, H., Wen, S., Huang, X., Song, C., Li, K., Wang, J., Keellings, D., and Lu, Y.: Human Activity Coupled With Climate Change Strengthens the Role of Lakes as an Active Pipe of Dissolved Organic Matter, Earths Future, 11, e2022EF003412, https://doi.org/10.1029/2022ef003412, 2023.

Evans, C. D., Freeman, C., Cork, L. G., Thomas, D. N., Reynolds, B., Billett, M. F., Garnett, M. H., and Norris, D.: Evidence against recent climate-induced destabilisation of soil carbon from ^{14}C analysis of riverine dissolved organic matter, Geophys. Res. Lett., 34, L07407, https://doi.org/10.1029/2007gl029431, 2007.

Fasching, C., Ulseth, A. J., Schelker, J., Steniczka, G., and Battin, T. J.: Hydrology controls dissolved organic matter export and composition in an Alpine stream and its hyporheic zone, Limnol. Oceanogr., 61, 558–571, https://doi.org/10.1002/lno.10232, 2016.

Fasching, C., Akotoye, C., Bižić, M., Fonvielle, J., Ionescu, D., Mathavarajah, S., Zoccarato, L., Walsh, D. A., Grossart, H. P., and Xenopoulos, M. A.: Linking stream microbial community functional genes to dissolved organic matter and inorganic nutrients, Limnol. Oceanogr., 65, S71–S87, https://doi.org/10.1002/lno.11356, 2019.

Fellman, J. B., Hood, E., and Spencer, R. G. J. L.: Fluorescence spectroscopy opens new windows into dissolved organic matter dynamics in freshwater ecosystems: A review, Limnol. Oceanogr., 55, 2452–2462, https://doi.org/10.4319/lo.2010.55.6.2452, 2010.

Fellman, J. B., Spencer, R. G., Raymond, P. A., Pettit, N. E., Skrzypek, G., Hernes, P. J., and Grierson, P. F.: Dissolved organic carbon biolability decreases along with its modernization in fluvial networks in an ancient landscape, Ecology, 95, 2622–2632, 2014.

Findlay, S., Sinsabaugh, R. L., Fischer, D. T., and Franchini, P.: Sources of dissolved organic carbon supporting planktonic bacterial production in the tidal freshwater Hudson River, Ecosystems, 1, 227–239, 1998.

Gaillardet, J., Dupre, B., Allegre, C. J., and Négrel, P.: Chemical and physical denudation in the Amazon River Basin, Chem. Geol., 142, 141–173, 1997.

Guo, L. B. and Gifford, R. M.: Soil carbon stocks and land use change: a meta analysis, Global Change Biol., 8, 345–360, https://doi.org/10.1046/j.1354-1013.2002.00486.x, 2002.

Han, G. and Liu, C.-Q.: Water geochemistry controlled by carbonate dissolution: a study of the river waters draining karst-dominated terrain, Guizhou Province, China, Chem. Geol., 204, 1–21, https://doi.org/10.1016/j.chemgeo.2003.09.009, 2004.

Harms, T. K., Edmonds, J. W., Genet, H., Creed, I. F., Aldred, D., Balser, A., and Jones, J. B.: Catchment influence on nitrate and dissolved organic matter in Alaskan streams across a latitudinal gradient, J. Geophys. Res.-Biogeo., 121, 350–369, https://doi.org/10.1002/2015jg003201, 2016.

He, W., Chen, M., Schlautman, M. A., and Hur, J.: Dynamic exchanges between DOM and POM pools in coastal and inland aquatic ecosystems: A review, Sci. Total Environ., 551–552, 415–428, https://doi.org/10.1016/j.scitotenv.2016.02.031, 2016.

Hengl, T., de Jesus, J. M., MacMillan, R. A., Batjes, N. H., Heuvelink, G. B., Ribeiro, E., Samuel-Rosa, A., Kempen, B., Leenaars, J. G., Walsh, M. G., and Gonzalez, M. R.: SoilGrids1km–global soil information based on automated mapping, PLOS ONE, 9, e105992, https://doi.org/10.1371/journal.pone.0105992, 2014.

Holt, A. D., Fellman, J., Hood, E., Kellerman, A. M., Raymond, P., Stubbins, A., Dittmar, T., and Spencer, R. G. M.: The evolution of stream dissolved organic matter composition following glacier retreat in coastal watersheds of southeast Alaska, Biogeochemistry, 164, 99–116, https://doi.org/10.1007/s10533-021-00815-6, 2021.

Hood, E., Fellman, J., Spencer, R. G., Hernes, P. J., Edwards, R., D'Amore, D., and Scott, D.: Glaciers as a source of ancient and labile organic matter to the marine environment, Nature, 462, 1044–1047, https://doi.org/10.1038/nature08580, 2009.

Hosen, J. D., McDonough, O. T., Febria, C. M., and Palmer, M. A.: Dissolved organic matter quality and bioavailability changes across an urbanization gradient in headwater streams, Environ. Sci. Technol., 48, 7817–7824, https://doi.org/10.1021/es501422z, 2014.

Inamdar, S., Singh, S., Dutta, S., Levia, D., Mitchell, M., Scott, D., Bais, H., and McHale, P.: Fluorescence characteristics and sources of dissolved organic matter for stream water during storm events in a forested mid-Atlantic watershed, J. Geophys. Res.-Biogeo., 116, G03043, https://doi.org/10.1029/2011jg001735, 2011.

Iwasaki, K., Nagasaka, Y., and Nagasaka, A.: Geological Effects on the Scaling Relationships of Groundwater Contributions in Forested Watersheds, Water Resour. Res., 57, e2021WR029641, https://doi.org/10.1029/2021wr029641, 2021.

Kadjeski, M., Fasching, C., and Xenopoulos, M. A.: Synchronous Biodegradability and Production of Dissolved Organic Matter in Two Streams of Varying Land Use, Front. Microbiol., 11, 568629, https://doi.org/10.3389/fmicb.2020.568629, 2020.

Kim, J., Kim, Y., Park, S. E., Kim, T. H., Kim, B. G., Kang, D. J., and Rho, T.: Impact of aquaculture on distribution of dissolved organic matter in coastal Jeju Island, Korea, based on absorption and fluorescence spectroscopy, Environ. Sci. Pollut. R. Int., 29, 553–563, https://doi.org/10.1007/s11356-021-15553-3, 2022.

Lambert, T., Pierson-Wickmann, A.-C., Gruau, G., Thibault, J.-N., and Jaffrezic, A.: Carbon isotopes as tracers of dissolved organic carbon sources and water pathways in headwater catchments, J. Hydrol., 402, 228–238, https://doi.org/10.1016/j.jhydrol.2011.03.014, 2011.

Lambert, T., Bouillon, S., Darchambeau, F., Morana, C., Roland, F. A. E., Descy, J.-P., and Borges, A. V.: Effects of human land use on the terrestrial and aquatic sources of fluvial organic matter in a temperate river basin (The Meuse River, Belgium), Biogeochemistry, 136, 191–211, https://doi.org/10.1007/s10533-017-0387-9, 2017.

Lambs, L.: Interactions between groundwater and surface water at river banks and the confluence of rivers, J. Hydrol., 288, 312–326, https://doi.org/10.1016/j.jhydrol.2003.10.013, 2004.

Lee, L.-C., Hsu, T.-C., Lee, T.-Y., Shih, Y.-T., Lin, C.-Y., Jien, S.-H., Hein, T., Zehetner, F., Shiah, F.-K., and Huang, J.-C.: Unusual roles of discharge, slope and soc in doc transport in small mountainous rivers, Taiwan, Sci. Rep., 9, 41422303, https://doi.org/10.1038/s41598-018-38276-x, 2019.

Leithold, E. L., Blair, N. E., and Perkey, D. W.: Geomorphologic controls on the age of particulate organic carbon from small mountainous and upland rivers, Global Biogeochem. Cy., 20, GB3022, https://doi.org/10.1029/2005gb002677, 2006.

Leonard, A., Castle, S., Burr, G. S., Lange, T., and Thomas, J.: A Wet Oxidation Method for AMS Radiocarbon Analysis of Dissolved Organic Carbon in Water, Radiocarbon, 55, 545–552, https://doi.org/10.1017/S0033822200057672, 2013.

Li, P., Lee, S. H., Lee, S. H., Lee, J. B., Lee, Y. K., Shin, H. S., and Hur, J.: Seasonal and storm-driven changes in chemical composition of dissolved organic matter: a case study of a reservoir and its forested tributaries, Environ. Sci. Pollut. R. Int., 23, 24834–24845, https://doi.org/10.1007/s11356-016-7720-z, 2016.

Li Yung Lung, J. Y. S., Tank, S. E., Spence, C., Yang, D., Bonsal, B., McClelland, J. W., and Holmes, R. M.: Seasonal and Geographic Variation in Dissolved Carbon Biogeochemistry of Rivers Draining to the Canadian Arctic Ocean and Hudson Bay, J. Geophys. Res.-Biogeo., 123, 3371–3386, https://doi.org/10.1029/2018jg004659, 2018.

Lloret, E., Dessert, C., Buss, H. L., Chaduteau, C., Huon, S., Alberic, P., and Benedetti, M. F.: Sources of dissolved organic carbon in small volcanic mountainous tropical rivers, examples from Guadeloupe (French West Indies), Geoderma, 282, 129–138, https://doi.org/10.1016/j.geoderma.2016.07.014, 2016.

Marwick, T. R., Tamooh, F., Teodoru, C. R., Borges, A. V., Darchambeau, F., and Bouillon, S.: The age of river-transported carbon: A global perspective, Global Biogeochem. Cy., 29, 122–137, https://doi.org/10.1002/2014GB004911, 2015.

Masiello, C. A. and Druffel, E. R.: Carbon isotope geochemistry of the Santa Clara River, Global Biogeochem. Cy., 15, 407–416, 2001.

Mayorga, E., Aufdenkampe, A. K., Masiello, C. A., Krusche, A. V., Hedges, J. I., Quay, P. D., Richey, J. E., and Brown, T. A.: Young organic matter as a source of carbon dioxide outgassing from Amazonian rivers, Nature, 436, 538–541, https://doi.org/10.1038/nature03880, 2005.

McDonough, L. K., Santos, I. R., Andersen, M. S., O'Carroll, D. M., Rutlidge, H., Meredith, K., Oudone, P., Bridgeman, J., Gooddy, D. C., Sorensen, J. P. R., Lapworth, D. J., MacDonald, A. M., Ward, J., and Baker, A.: Changes in global groundwater organic carbon driven by climate change and urbanization, Nat. Commun., 11, 1279, https://doi.org/10.1038/s41467-020-14946-1, 2020.

McGuire, K. J., McDonnell, J. J., Weiler, M., Kendall, C., McGlynn, B. L., Welker, J. M., and Seibert, J.: The role of topography on catchment-scale water residence time, Water Resour. Res., 41, W05002, https://doi.org/10.1029/2004wr003657, 2005.

McKnight, D. M., Boyer, E. W., Westerhoff, P. K., Doran, P. T., Kulbe, T., and Andersen, D. T.: Spectrofluorometric characterization of dissolved organic matter for indication of precursor organic material and aromaticity, Limnol. Oceanogr., 46, 38–48, https://doi.org/10.4319/lo.2001.46.1.0038, 2001.

Meybeck, M.: Atmospheric inputs and river transport of dissolved substance, edited by: Webb, B. W., Dissolved loads of Rivers and Surface Water Quantity/Quality Relationships. IAHS, Hamburg, 173–192, 1983.

Minor, E. C., Swenson, M. M., Mattson, B. M., and Oyler, A. R.: Structural characterization of dissolved organic matter: a review of current techniques for isolation and analysis, Environ. Sci. Processes Impacts, 16, 2064–2079, https://doi.org/10.1039/c4em00062e, 2014.

Montgomery, D. R.: Soil erosion and agricultural sustainability, P. Natl. Acad. Sci. USA, 104, 13268–13272, https://doi.org/10.1073/pnas.0611508104, 2007.

Mostofa, K. M. G., Jie, Y., Sakugawa, H., and Liu, C. Q.: Equal Treatment of Different EEM Data on PARAFAC Modeling Produces Artifact Fluorescent Components That Have Misleading Biogeochemical Consequences, Environ. Sci. Technol., 53, 561–563, https://doi.org/10.1021/acs.est.8b06647, 2019.

Moyer, R. P., Bauer, J. E., and Grottoli, A. G.: Carbon isotope biogeochemistry of tropical small mountainous river, estuarine, and coastal systems of Puerto Rico, Biogeochemistry, 112, 589–612, https://doi.org/10.1007/s10533-012-9751-y, 2013.

Murphy, K. R., Stedmon, C. A., Wenig, P., and Bro, R.: OpenFluor–an online spectral library of auto-fluorescence by organic compounds in the environment, Anal. Methods-UK, 6, 658–661, 2014.

Mzobe, P., Yan, Y., Berggren, M., Pilesjö, P., Olefeldt, D., Lundin, E., Roulet, N. T., and Persson, A.: Morphometric Control on Dissolved Organic Carbon in Subarctic Streams, J. Geophys. Res.-Biogeo., 125, e2019JG005348, https://doi.org/10.1029/2019jg005348, 2020.

Nagy, R. C., Porder, S., Brando, P., Davidson, E. A., Figueira, A., Neill, C., Riskin, S., and Trumbore, S.: Soil Carbon Dynamics in Soybean Cropland and Forests in Mato Grosso, Brazil, J. Geophys. Res.-Biogeo., 123, 18–31, https://doi.org/10.1002/2017JG004269, 2018.

Neff, J. C., Finlay, J. C., Zimov, S. A., Davydov, S. P., Carrasco, J. J., Schuur, E. A. G., and Davydova, A. I.: Seasonal changes in the age and structure of dissolved organic carbon in Siberian rivers and streams, Geophys. Res. Lett., 33, L23401, https://doi.org/10.1029/2006gl028222, 2006.

Nkoue Ndondo, G. R., Probst, J. L., Ndjama, J., Ndam Ngou-payou, J. R., Boeglin, J. L., Takem, G. E., Brunet, F., Mortatti, J., Gauthier-Lafaye, F., Braun, J. J., and Ekodeck, G. E.: Stable Carbon Isotopes δ^{13}C as a Proxy for Characterizing Carbon Sources and Processes in a Small Tropical Headwater Catchment: Nsimi, Cameroon, Aquat. Geochem., 27, 1–30, https://doi.org/10.1007/s10498-020-09386-8, 2020.

Ohno, T.: Fluorescence inner-filtering correction for determining the humification index of dissolved organic matter, Environ. Sci. Technol., 36, 742–746, https://doi.org/10.1021/es0155276, 2002.

Opsahl, S. P. and Zepp, R. G.: Photochemically-induced alteration of stable carbon isotope ratios (δ^{13}C) in terrigenous dissolved organic carbon, Geophys. Res. Lett., 28, 2417–2420, https://doi.org/10.1029/2000gl012686, 2001.

Paerl, H. W.: Controlling Eutrophication along the Freshwater–Marine Continuum: Dual Nutrient (N and P) Reductions are Essential, Estuar. Coast., 32, 593–601, https://doi.org/10.1007/s12237-009-9158-8, 2009.

Palmer, S. M., Hope, D., Billett, M. F., Dawson, J. J., and Bryant, C. L.: Sources of organic and inorganic carbon in a headwater stream: evidence from carbon isotope studies, Biogeochemistry, 52, 321–338, 2001.

Parlanti, E., Wörz, K., Geoffroy, L., and Lamotte, M.: Dissolved organic matter fluorescence spectroscopy as a tool to estimate biological activity in a coastal zone submitted to anthropogenic inputs, Org. Geochem., 31, 1765–1781, https://doi.org/10.1016/S0146-6380(00)00124-8, 2000.

Poulin, B. A., Ryan, J. N., and Aiken, G. R.: Effects of iron on optical properties of dissolved organic matter, Environ. Sci. Technol., 48, 10098–10106, https://doi.org/10.1021/es502670r, 2014.

Quinton, J. N., Govers, G., Van Oost, K., and Bardgett, R. D.: The impact of agricultural soil erosion on biogeochemical cycling, Nat. Geosci., 3, 311–314, https://doi.org/10.1038/ngeo838, 2010.

Ramos, M. C., Quinton, J. N., and Tyrrel, S. F.: Effects of cattle manure on erosion rates and runoff water pollution by faecal coliforms, J. Environ. Manage., 78, 97–101, https://doi.org/10.1016/j.jenvman.2005.04.010, 2006.

Rawlins, M. A., Connolly, C. T., and McClelland, J. W.: Modeling Terrestrial Dissolved Organic Carbon Loading to Western Arctic Rivers, J. Geophys. Res.-Biogeo., 126, e2021JG006420, https://doi.org/10.1029/2021jg006420, 2021.

Raymond, P. A. and Spencer, R. G. M.: Chapter 11 – Riverine DOM, in: Biogeochemistry of Marine Dissolved Organic Matter, second edition, edited by: Hansell, D. A. and Carlson, C. A., Academic Press, Boston, 509–533, ISBN 978-0-12-405940-5, 2015.

Raymond, P. A., Bauer, J. E., Caraco, N. F., Cole, J. J., Longworth, B., and Petsch, S. T.: Controls on the variability of organic matter and dissolved inorganic carbon ages in northeast US rivers, Mar. Chem., 92, 353–366, https://doi.org/10.1016/j.marchem.2004.06.036, 2004.

Raymond, P. A., Hartmann, J., Lauerwald, R., Sobek, S., McDonald, C., Hoover, M., Butman, D., Striegl, R., Mayorga, E., Humborg, C., Kortelainen, P., Durr, H., Meybeck, M., Ciais, P., and Guth, P.: Global carbon dioxide emissions from inland waters, Nature, 503, 355–359, https://doi.org/10.1038/nature12760, 2013.

Ryan, K. A., Palacios, L. C., Encina, F., Graeber, D., Osorio, S., Stubbins, A., Woelfl, S., and Nimptsch, J.: Assessing inputs of aquaculture-derived nutrients to streams using dissolved organic matter fluorescence, Sci. Total Environ., 807, 150785, https://doi.org/10.1016/j.scitotenv.2021.150785, 2022.

Sanchez, G.: PLS path modeling with R, Trowchez Editions, Berkeley, 383, 551, http://www.gastonsanchez.com/PLSPathModelingwithR.pdf (last access: 25 October 2023), 2013.

Schiff, S. L., Aravena, R., Trumbore, S. E., Hinton, M. J., Elgood, R., and Dillon, P. J.: Export of DOC from forested catchments on the Precambrian Shield of Central Ontario: Clues from ^{13}C and ^{14}C, Biogeochemistry, 36, 43–65, 1997.

Shen, Y., Chapelle, F. H., Strom, E. W., and Benner, R.: Origins and bioavailability of dissolved organic matter in groundwater, Biogeochemistry, 122, 61–78, https://doi.org/10.1007/s10533-014-0029-4, 2015.

Shutova, Y., Baker, A., Bridgeman, J., and Henderson, R. K.: Spectroscopic characterisation of dissolved organic matter changes in drinking water treatment: From PARAFAC analysis to online monitoring wavelengths, Water Res., 54, 159–169, https://doi.org/10.1016/j.watres.2014.01.053, 2014.

Sickman, J. O., Zanoli, M. J., and Mann, H. L.: Effects of Urbanization on Organic Carbon Loads in the Sacramento River, California, Water Resour. Res., 43, W11422, https://doi.org/10.1029/2007wr005954, 2007.

Smith, V. H. and Schindler, D. W.: Eutrophication science: where do we go from here?, Trends Ecol. Evol., 24, 201–207, https://doi.org/10.1016/j.tree.2008.11.009, 2009.

Song, C., Wang, G., Haghipour, N., and Raymond, P. A.: Warming and monsoonal climate lead to large export of millennial-aged carbon from permafrost catchments of the Qinghai–Tibet Plateau, Environ. Res. Lett., 15, 074012, https://doi.org/10.1088/1748-9326/ab83ac, 2020.

Spencer, R. G. M., Guo, W., Raymond, P. A., Dittmar, T., Hood, E., Fellman, J., and Stubbins, A.: Source and biolability of ancient dissolved organic matter in glacier and lake ecosystems on the Tibetan Plateau, Geochim. Cosmochim. Ac., 142, 64–74, https://doi.org/10.1016/j.gca.2014.08.006, 2014.

Spencer, R. G. M., Kellerman, A. M., Podgorski, D. C., Macedo, M. N., Jankowski, K., Nunes, D., and Neill, C.: Identifying the Molecular Signatures of Agricultural Expansion in Amazonian Headwater Streams, J. Geophys. Res.-Biogeo., 124, 1637–1650, https://doi.org/10.1029/2018jg004910, 2019.

Stanley, E. H., Powers, S. M., Lottig, N. R., Buffam, I., and Crawford, J. T.: Contemporary changes in dissolved organic carbon (DOC) in human-dominated rivers: is there a role for DOC management?, Freshwater Biol., 57, 26–42, https://doi.org/10.1111/j.1365-2427.2011.02613.x, 2012.

Stedmon, C. A. and Bro, R.: Characterizing dissolved organic matter fluorescence with parallel factor analysis: a tutorial, Limnol. Oceanogr.-Meth., 6, 572–579, https://doi.org/10.4319/lom.2008.6.572, 2008.

Tian, J., Dungait, J. A. J., Lu, X., Yang, Y., Hartley, I. P., Zhang, W., Mo, J., Yu, G., Zhou, J., and Kuzyakov, Y.: Long-term nitrogen addition modifies microbial composition and functions for slow carbon cycling and increased sequestration in tropical forest soil, Global Change Biol., 25, 3267–3281, https://doi.org/10.1111/gcb.14750, 2019.

Tittel, J., Büttner, O., Freier, K., Heiser, A., Sudbrack, R., and Ollesch, G.: The age of terrestrial carbon export and rainfall intensity in a temperate river headwater system, Biogeochemistry, 115, 53–63, https://doi.org/10.1007/s10533-013-9896-3, 2013.

Toming, K., Tuvikene, L., Vilbaste, S., Agasild, H., Viik, M., Kisand, A., Feldmann, T., Martma, T., Jones, R. I., and Nõges, T.: Contributions of autochthonous and allochthonous sources to dissolved organic matter in a large, shallow, eutrophic lake with a highly calcareous catchment, Limnol. Oceanogr., 58, 1259–1270, https://doi.org/10.4319/lo.2013.58.4.1259, 2013.

Veum, K. S., Goyne, K. W., Motavalli, P. P., and Udawatta, R. P.: Runoff and dissolved organic carbon loss from a paired-watershed study of three adjacent agricultural Watersheds, Agr. Ecosyst. Environ., 130, 115–122, https://doi.org/10.1016/j.agee.2008.12.006, 2009.

Vonk, J. E. and Gustafsson, Ö.: Permafrost-carbon complexities, Nat. Geosci., 6, 675–676, https://doi.org/10.1038/ngeo1937, 2013.

Voss, B. M., Peucker-Ehrenbrink, B., Eglinton, T. I., Spencer, R. G. M., Bulygina, E., Galy, V., Lamborg, C. H., Ganguli, P. M., Montluçon, D. B., Marsh, S., Gillies, S. L., Fanslau, J., Epp, A., and Luymes, R.: Seasonal hydrology drives rapid shifts in the flux and composition of dissolved and particulate organic carbon and major and trace ions in the Fraser River, Canada, Biogeosciences, 12, 5597–5618, https://doi.org/10.5194/bg-12-5597-2015, 2015.

Voss, B. M., Eglinton, T. I., Peucker-Ehrenbrink, B., Galy, V., Lang, S. Q., McIntyre, C., Spencer, R. G. M., Bulygina, E., Wang, Z. A., and Guay, K. A.: Isotopic evidence for sources of dissolved carbon and the role of organic matter respiration in the Fraser River basin, Canada, Biogeochemistry, 164, 207–228, https://doi.org/10.1007/s10533-022-00945-5, 2022.

Walker, S. A., Amon, R. M. W., Stedmon, C., Duan, S., and Louchouarn, P.: The use of PARAFAC modeling to trace terrestrial dissolved organic matter and fingerprint water masses in coastal Canadian Arctic surface waters, J. Geophys. Res., 114, G00F06, https://doi.org/10.1029/2009jg000990, 2009.

Wang, J., Walter, B. A., Yao, F., Song, C., Ding, M., Maroof, A. S., Zhu, J., Fan, C., McAlister, J. M., Sikder, S., Sheng, Y., Allen, G. H., Crétaux, J.-F., and Wada, Y.: GeoDAR: georeferenced global dams and reservoirs dataset for bridging attributes and geolocations, Earth Syst. Sci. Data, 14, 1869–1899, https://doi.org/10.5194/essd-14-1869-2022, 2022.

Weishaar, J. L., Aiken, G. R., Bergamaschi, B. A., Fram, M. S., Fujii, R., and Mopper, K.: Evaluation of specific ultraviolet absorbance as an indicator of the chemical composition and reactivity of dissolved organic carbon, Environ. Sci. Technol., 37, 4702–4708, 2003.

Williams, C. J., Yamashita, Y., Wilson, H. F., Jaffé, R., and Xenopoulos, M. A.: Unraveling the role of land use and microbial activity in shaping dissolved organic matter characteristics in stream ecosystems, Limnol. Oceanogr., 55, 1159–1171, https://doi.org/10.4319/lo.2010.55.3.1159, 2010.

Williams, C. J., Frost, P. C., Morales-Williams, A. M., Larson, J. H., Richardson, W. B., Chiandet, A. S., and Xenopoulos, M. A.: Human activities cause distinct dissolved organic matter composition across freshwater ecosystems, Global Change Biol., 22, 613–626, https://doi.org/10.1111/gcb.13094, 2016.

Wilson, H. F. and Xenopoulos, M. A.: Effects of agricultural land use on the composition of fluvial dissolved organic matter, Nat. Geosci., 2, 37–41, https://doi.org/10.1038/ngeo391, 2008.

Xenopoulos, M. A., Barnes, R. T., Boodoo, K. S., Butman, D., Catalán, N., D'Amario, S. C., Fasching, C., Kothawala, D. N., Pisani, O., Solomon, C. T., Spencer, R. G. M., Williams, C. J., and Wilson, H. F.: How humans alter dissolved organic matter composition in freshwater: relevance for the Earth's biogeochemistry, Biogeochemistry, 1–26, https://doi.org/10.1007/s10533-021-00753-3, 2021.

Yi, Y., Zhong, J., Bao, H., Mostofa, K. M. G., Xu, S., Xiao, H.-Y., and Li, S.-L.: The impacts of reservoirs on the sources and transport of riverine organic carbon in the karst area: a multi-tracer study, Water Res., 194, 116933, https://doi.org/10.1016/j.watres.2021.116933, 2021.

Yi, Y., Li, S.-L., Zhong, J., Wang, W., Chen, S., Bao, H., and He, D.: The influence of the deep subtropical reservoir on the karstic riverine carbon cycle and its regulatory factors: Insights from the seasonal and hydrological changes, Water Res., 226, https://doi.org/10.1016/j.watres.2022.119267, 2022.

Zhang, Q., Tao, Z., Ma, Z., Gao, Q., Deng, H., Xu, P., Ding, J., Wang, Z., and Lin, Y.: Hydro-ecological controls on riverine organic carbon dynamics in the tropical monsoon region, Sci. Rep., 9, 11871, https://doi.org/10.1038/s41598-019-48208-y, 2019.

Zhang S., Yin, Y., Yang, P., Yao, C., Tian, S., Lei, P., Jiang, T., and Wang, D.: Using the end-member mixing model to evaluate biogeochemical reactivities of dissolved organic matter (DOM): autochthonous versus allochthonous origins, Water Res., 232, 119644, https://doi.org/10.1016/j.watres.2023.119644, 2023.

Zhong, J., Chen, S., Wang, W., Yan, Z., Ellam, R. M., and Li, S. L.: Unravelling the hydrological effects on spatiotemporal variability of water chemistry in mountainous rivers from Southwest China, Hydrol. Process., 34, 5595–5605, https://doi.org/10.1002/hyp.13980, 2020.

Zhong, J., Li, S.-L., Zhu, X., Liu, J., Xu, S., Xu, S., and Liu, C.-Q.: Dynamics and fluxes of dissolved carbon under short-term climate variabilities in headwaters of the Changjiang River, draining the Qinghai–Tibet Plateau, J. Hydrol., 596, 126128, https://doi.org/10.1016/j.jhydrol.2021.126128, 2021.

Zhou, Y., Davidson, T. A., Yao, X., Zhang, Y., Jeppesen, E., de Souza, J. G., Wu, H., Shi, K., and Qin, B.: How autochthonous dissolved organic matter responds to eutrophication and climate warming: Evidence from a cross-continental data analysis and experiments, Earth-Sci. Rev., 185, 928–937, https://doi.org/10.1016/j.earscirev.2018.08.013, 2018.

Zhou, Y., Yao, X., Zhou, L., Zhao, Z., Wang, X., Jang, K. S., Tian, W., Zhang, Y., Podgorski, D. C., Spencer, R. G. M., Kothawala, D. N., Jeppesen, E., and Wu, F.: How hydrology and anthropogenic activity influence the molecular composition and export of dissolved organic matter: Observations along a large river continuum, Limnol. Oceanogr., 66, 1730–1742, https://doi.org/10.1002/lno.11716, 2021.